Sensitivity and performance evaluation of full basin weekly average sampling strategy for Ocean Color

MFSTEP WP6-D11

G. Crispi and M. Pacciaroni, Istituto Nazionale di Oceanografia e di Geofisica Sperimentale–OGS

OGS REPORT 30/2006 - OGA15

Trieste, May 2006

INDEX:

Keywords: nitrogen, ecosystem modeling, reduced-order optimal interpolation, twin experiments, data assimilation, chlorophyll, Mediterranean Sea.

1. Introduction

Ecosystem 3-D general circulation description of the ecological processes at one eighth of degree is determined by means of GCM-NPZD balanced ecomodel, based on Nitrate, N, Phytoplankton, P, Zooplankton, Z, and Detritus, D (MFSTEP WP6-D5, 2004).

A reciprocal interaction between the elemental composition of marine biota and their dissolved nutrition resources is assumed, whereby the nutrient elements are taken up and released in fixed proportions of C:N:P of 106:16:1. It is assumed that the biological production in the ocean is principally limited by the availability of nitrogen, meaning that the supply of nitrogen also determines the amount of carbon incorporated into biomass. Production based on nitrate, which newly enters the euphotic zone, where light availability is sufficient for net growth, is referred to as new production and is differentiated from production based on the remineralized compounds of nitrogen.

The aim of simulating relevant biological processes has led to the development of nitrogen-based models of marine ecosystems. Such models were coupled to basin-scale general circulation models - GCM - of the Mediterranean Sea (Demirov and Pinardi, 2002). Such models simply transfer mass from an inorganic reservoir into organic pools and may lack, for instance, important ecological processes. These biological models include parameterisations mostly describing mass exchange rates. In general the model parameters are considered to be constant in time. Hence, the model solutions strongly depend on the choice of the corresponding biological parameters which, in addition, need to represent a diversity of individual organisms, grouped into compartments of, for example, phytoplankton and herbivorous zooplankton. Since the model parameters should represent a complex system in such a simple way, their appropriate estimate remains a major challenge.

The optimal interpolation system is SOFA - System for Ocean Forecasting and Interpolation 3.0 version (build 284) - tested, optimized and set up for identical twin experiments - ITE - based on phytoplankton biomass in nitrogen units. ITE have been performed on IBM-SP4-AIX 5.1 with 48 nodes assimilating biomass data in univariate mode. After porting the integrated system on IBM-SP5 AIX 5.2 with 512 Power 5, it has been used for fraternal twin experiments – FTE - based on Ocean Color in chlorophyll units. This version, ported from SGI to IBM, is optimized and modified for biomass data assimialtion.

The control run is assumed to be for both environments a true ecosystem evolution. Therefore, simulated observations of chlorophyll are extracted from the respective control "sea-truth" in terms of weekly averages of full basin coverage at the level 3 of Ocean Color. The fraternal assimilation run is based on the GCM-NPZD eco-hydrodynamical model with similar physics but aggregated biology. The assimilation procedure is proven successful both for surface biomass optimally interpolated once a week and in the case of surficial chlorophyll assimilated at the same time scale.

Ecological processes

Plankton represents the first step in the food web of the ocean and of fresh water, and components of the plankton are food for many of the fish harvested by humans. Plankton play a major role in cycling of chemical elements in the ocean, and thereby also affects the chemical composition of sea water, through exchange of gases between the sea and the atmosphere. In the parts of the ocean where plankton is abundant, this is the cause for major contributions to deep-sea sediments.

Although horizontal movement of plankton at kilometer scales is passive, the metazooplankton perform vertical migrations on scales of 10-100 m. This vertical range can displace them from the near surface lighted waters, where the phytoplankton grows, to darker and colder environments.

The plankton can be subdivided along functional lines and in terms of size. The size category, picoplankton (0.2-2.0 μm), is approximately equivalent to the functional category, bacterioplankton; most phytoplankton, nanoplankton and netplankton, and protozooplankton, single-celled animals, are 2.0-20 μm and 20-200 μm, respectively.

Depending on sunlight for photosynthesis, plankton lives from the surface to 50-200 m of the ocean – within the euphotic depth. Nutrients such as nitrate and phosphate are incorporated into protoplasm in company with photosynthesis, and returned to dissolved form by excretion or remineralization of dead organic matter called detritus. Since much of the remineralization occurs after sinking of the detritus, uptake of nutrients and their regeneration are partially separated vertically. Whenever photosynthesis is proceeding actively and vertical mixing is not excessive, a near surface layer of low nutrient concentrations is separated from a layer of abundant nutrients, some distance below the euphotic depth, by the nutricline, layer in which nutrient concentrations increase strongly with depth. The spatial and temporal relations between euphotic depth, nutricline, and pycnocline are important determinants of the productivity of phytoplankton.

Zooplankton is typically concentrated within the euphotic zone; because of sinking of detritus and vertical migration, various types of zooplankton can be found at different depths in the ocean.

The distribution of planktonic species is dependent on currents, thus species are not uniformly distributed throughout the ocean and tend to be confined to particular water masses, with average physiological characteristics and specific interactions with other species of the trophic chain.

Primary production and its distribution

Primary production is the synthesis of organic material from inorganic compounds, such as CO_2 and water, a carbon fixation process: CO_2 is fixed both by

chemosynthesis and by photosynthesis, which accounts for most marine primary production.

Primary producers, such as marine phytoplankton and marine benthic are organisms, that rely on external energy sources such as light energy or inorganic chemicals reactions. These organisms are further characterized by obtaining their elemental requirements from inorganic sources, e.g. carbon from inorganic carbon such as carbon dioxide and bicarbonate, nitrogen from nitrate and ammonium, and phosphorus from inorganic phosphate. These organisms form the basis of food webs, supporting all organisms at higher trophic levels.

In studying the distribution of primary production in the ocean, one has to plan measurements at time and space scales appropriate for the problem at hand. The carbon-based measured quantities are gross primary production, and net primary production; the nitrogen-base ones are total production, new production, and regenerated production.

The light field varies with depth in the ocean, with time of one day, the diel variation, and with time of one year, the yearly variation. Correspondingly, primary production in the ocean exhibits a strong depth dependence and a strong time dependence. The temporal variations occur on several scales, ranging from seconds, response to clouds and vertical mixing, to diurnal, seasonal, and annual. Adaptations of phytoplankton populations to various light regimes influence primary production. The adaptation may involve changes: in the concentration of chlorophyll–a per cell; in the number of chlorophyll-a molecules per photosynthetic unit; in the concentrations of auxiliary pigments, introducing some internal cell variable taking into account the history of the cell.

It has been a common practice, and here we follow it, to treat the concentration of the main phytoplankton pigment, chlorophyll-a, as an index of phytoplankton biomass, because it is present in all types of phytoplankton, it is easy to measure, and of the fundamental role it plays in the photosynthetic process. Light acts on the state

variable, the biomass of phytoplankton, and as limiting factor of the primary production.

Another factor limiting the primary production in the ocean is the availability of essential nutrients such as nitrogen. In a stratified, oceanic water column, the upper illuminated layer is typically low in nutrients, with the deeper layers acting as a reservoir of nutrients. Mixing events bring these nutrients to the surface layer, enhancing primary production. In temperate and high latitudes, deep mixing events in winter, and subsequent stratification as the surface warming trend begins, lead to the well-known phenomenon of the spring bloom and more generally to pronounced seasonal cycle in primary production.

The recent years have seen an increasing appreciation of the role of micronutrients such as iron as limiting resources for primary production. However, it is not a Mediterranean peculiarity but the Southern Ocean, the Equatorial Pacific, the subarctic Pacific one.

Other contributing factors for the presence of high nutrient, low-chlorophyll regimes include top-down control of phytoplankton biomass, and hence productivity, by zooplankton grazing, and the supply of nutrients by physical processes that exceeds the demands of biological production.

In view of the large number of factors that influence the distribution of primary production at so many temporal and spatial scales, it is convenient to apply mathematical modeling techniques to organize and formalize the study of the distribution of primary production in the world oceans. Light-dependent models of primary production are especially suitable since are on basic principles of plant physiology and also because can take advantage of information obtained by remote sensing of quantities related to abundance of phytoplankton at sea surface.

It is only the upper part of the water column that contributes to primary production. Moreover phytoplankton themselves are a major factor responsible for modifying the optical properties of sea water, and the rate of penetration of solar radiation into the ocean.

Useful depth horizon that is relevant in the study of primary production is the critical depth. If production and loss terms of phytoplankton - grazing, sinking, decay - from the surface to some finite dept are integrated, then the integrated production and loss terms become equal to each other at some depth of integration, which is known as the critical depth. The concept of critical depth was formalized by Sverdrup in 1956. If the mixed-layer depth is shallower than the critical depth, then production in the layer will exceed losses, which is favorable for the accumulation of biomass in the layer. If the mixed-layer depth is deeper than the critical depth, the conditions would be unfavorable for the formation of blooms.

In fact, the maximum primary production may well occur at some subsurface depth, where the nutrient availability and light levels are optimal.

Primary production varies markedly with region and with season. Upwelling regions, e.g., waters off north-west Africa, the north-west Arabian Sea off Somalia, the equatorial divergence zone, the north-east Pacific off California and Oregon, the south-east Pacific off Peru, and south-west Africa, are typically more productive than the central gyres of the major oceans basins, because of the high levels of nutrients that are brought to the surface by upwelling. In general, coastal regions are more productive than open-ocean waters, due to an higher availability of nutrients.

Mediterranean biochemical characteristics and modeling

Analysis of existing biochemical datasets, collected using different techniques, confirms biochemical peculiarities of the Mediterranean Sea. These datasets exhibit the following peculiarities regarding nutrients:

1. an extreme open-sea oligotrophy in comparison with main oceans;
2. a huge spatial variability with maxima in coastal areas, due to river run-off and/or anthropic pressure;
3. significant seasonal excursion with variations comparable to the average values.

The inverse estuarine circulation of the whole basin creates a negative budget for the nutrients at the Gibraltar Strait (Coste et al., 1988), importing nutrient poor surface water from the Atlantic Ocean and exporting into it relatively nutrient-rich intermediate water.

Permanent and recurrent gyres, mainly cyclonic in the northern area of the basin and anticyclonic in the southern one, affect the vertical advection of nutrients, the main factor for new production.

Thus a model analysis of the Mediterranean ecosystem variability must take into account the detailed hydrodynamics of the basin, which can be done by coupling a model of the biochemical processes with a 3-D hydrodynamics model of the entire basin.

Primary production in the Mediterranean ecosystem is limited both by the nutrient availability, conditioned by physical oceanographic processes at different time and space scales, and by irradiance and its light penetration in the water column.

The Mediterranean Sea has been studied from the ecological point of view since recent years. Some areas, or "regions", were considered as well as the whole Mediterranean basin by various models.

A distinction of the ecomodels can be done in terms of spatial dimensionality, which is very important for the bind of imposed fluxes at the boundaries: zero-dimensional models where all parameters are mixed and homogeneity is assumed; one-dimensional models taking into account vertical processes, but disregarding lateral fluxes and diffusions; finally three-dimensional models used for studying limited-area or regional evolution but also for the coverage of all the Mediterranean area.

Another distinction depends on the complexity of the biochemical description: few compartments give a basic picture of the ecosystem evolution; an aggregated description with some capacity in following the cycles of the carbon and of the nutrients; versions of the ecosystem relations more resolved in term of functional relations.

Another point is the importance of the turbulence parameterization, representing the mixing processes. Different schemes of vertical turbulent diffusion can be considered for the biochemistry. In the oceanographic literature there are many examples where the vertical eddy diffusivity is approximated through a constant vertical parameterization. There are also models with a proposed Richardson-number vertical diffusivity estimates, k-ε and Mellor-Yamada schemes.

The last two decades of the twentieth century saw the development of remote sensing techniques to study the distribution of phytoplankton in the ocean. This technology uses subtle variations in the color of the oceans, as monitored by a sensor aboard satellites, to quantify variations in the concentration of chlorophyll-a in the surface layers of the ocean. Since polar-orbiting satellites' swaths cover the globe at high spatial resolution (1 km or better), it is possible to see in great wealth of detail the variations in phytoplankton distribution at synoptic scales. The next logical step in the exploitation of ocean color data was taken a few years later, when these fields of biomass were converted into fields of primary production. On this innovations are based the improvements of models describing photosynthesis as a function of available light.

The aim of this work is to evaluate the feasibility, the efficiency and the limits of the assimilation of superficial chlorophyll data in view of possible activities in operational oceanography. Assessing the potential improvement of basin scale ecosystem predictions for the Mediterranean Sea adopting data assimilation strategies for ocean-color data is the theme of the Observing System Simulation Experiments proposed here. They provide the quantitative basis for a rationale design of subsurface observing systems that have to complement the information from the satellite ocean colour.

The most successful procedure relies on models of the photosynthesis as a function of the photosynthetic available radiation and of the nutrient cycling. Thus the light available at the sea surface is estimated in this work using optimization methods and the nitrogen limitation is traced dynamically.

The numerical experiments are based upon an established ecosystem model set up in the frame of the European-Commission Mediterranean Targeted Projects 1 (Pinardi et al., 1997) and 2 (Monaco and Peruzzi, 2002). The model has moderated biological complexity to be used in tight coupling with the assimilation scheme. Moreover there is experience that such a model can capture the main biogeochemical fluxes characteristics of the Mediterranean basins: oligotrophy, seasonal cycle, biological gradients.

Reliable model data of the phytoplankton, P, from ECHYM have been used in the data assimilation process with the nudging scheme. Via Newtonian relaxation procedure, the P values were assimilated at the first computational layer, 10 meters from the sea surface of the MOM-NPZD model. Three different time-relaxation parameters were used: 5 days - also used for the relaxation of surface salinity boundary conditions to the climatological monthly mean values - , 1 day and 0.5 day. The comparison of the simulation results obtained with the nudging schemes shows an increase of the calculated biomass, because of the biomass assimilation (Crispi et al., 2003).

In the frame of the study of the interaction among hydrodynamical processes and ecological systems, a quantitative interpretation of the biogeochemistry in the Ionian Sea and of the seasonal variability of the nitrogen cycles in Mediterranean has been gained. In the Ionian Sea the trophic web is dominated by the nutrient regeneration. This mechanism releases the dissolved organic phase in the inorganic one, which is immediately reusable by primary living organisms. Results of the Ionian model are taken after spin-up of the hydrodynamics forty-five months long (Civitarese et al., 1996). The initialization was based on the chemical data gathered during the cruise POEM-BC-O91, while the biology was initialized with an average of measured profiles. As a result, the dynamics of phytoplankton depended both on the nitrogen flux coming from the Sicily Strait and on the vertical movements due to gyres and upwellings. Estimate of the primary production was in good accord with the one obtained on the basis of consumed oxygen. The climatological influence of

the general circulation on the nutrient distribution was evident in permanent cyclonic areas, while anticyclonic areas did not give valuable signals because of the oligotrophy of the superficial layer.

Thus basic trophodynamics coupled with the general circulation can reproduce biological and ecological main features of the oligotrophic marine environment like Ionian subbasin. In the present MFSTEP Project a similar integrated approach is followed maintaining fixed properties and characteristic parameters of plankton, while the available nitrogen is the only free evolving nutrient.

Ecosystem description concerning the general circulation with the 3D GCM - set up according with the parameterization chosen during the MFSPP Project (Demirov and Pinardi, 2002) - has been set up by means of NPZD model. This model describes both the primary trophic cycles and the nearly balanced chemical evolution (Crispi and Pacciaroni, 2005). Several simulations of different spanning times have been carried out. They give the space and time evolution of N, P, Z, and D reaching their seasonal cycles, starting from homogeneous initial conditions. The different oligotrophy of the Mediterranean basins is demonstrated in the long-run, i. e. in more than thirty-three years simulation, by the total nitrogen in the upper layer, in the intermediate layer and in overall content.

The system of optimal interpolation used for this ecosystem is the SOFA-System for Ocean Forecasting and Interpolation 3.0 version-build 284 (De Mey and Benkiran, 2002), as used during Preliminary Phase of MFS for assimilating various strategies of XBT, expendable bathythermograph, at VOS, volunteer observing ship tracks, airborne XBT and SST (Raicich and Rampazzo, 2003). It uses temperature and salinity as tracers and possibly assimilates also streamfunction. The system has been ported, customized and tested on the CINECA 48 nodes supercomputer SP4-AIX 5.1. The required ESSL and LAPACK libraries have been substituted on this machine by the optimized MASS library. Execution time is about four minutes for the integrated system, i. e. assimilation plus hydrodynamics plus biochemistry. The running time is one day with timestep of 900 s.

This version is optimized and the interface is modified for assimilating biomass data. The NPZD model evolution from the 1st September to the 29th December 1998 is the originator of the assimilated data. Identical Twin Experiments (ITE) are performed changing the initial conditions of the phytoplankton biomass and assimilating at the end of the week the averaged biomass of the past week at 5 m and at 15 m levels.

The twin experiments start after dynamical adjustment from the 1st of September to the 28th of December of the 1998 year, considered as perpetual year. The forcing functions in the experiment are daily forcing, and span from the December 29 to the March 8. Seven days averages of the Reference Run P are used in the optimal interpolation process at the end of each weekly synthetic acquisition period. This procedure induces the name of identical – i. e. control data generated by the same ecomodel – in the twin experiment procedure.

In Figure 1.1 the phytoplankton, after averaging its biomass in nitrogen units, is shown. The three runs basin averages – Reference Run (non-assimilated and unperturbed run), Free Run (non-assimilated and re-initialized with summer biomass), Assimilation Run (assimilated and re-initialized with summer biomass) – are given during the evolution.

In the Reference Run, total phytoplankton increases from the initial value, reached at the end of the adjustment period, toward higher values, and, after these maxima obtained approximately at the end of February, it decreases. The Free Run gives a completely different behaviour: starting from quite low values, due to the summer biomass conditions injected at the beginning of the run, it has a very fast step in the first 40 days toward maxima of the same order in the Reference Run; at the end of the simulation period, distinct higher values are attained. In the Assimilation Run, the steps toward maxima every seven days, i. e. at assimilation times, are even more pronounced than in the Free Run, getting facilities from the statistical optimal interpolation procedure; in every case, at the end of the twin experiments lower

values than Free Run ones are reached. Thus the biomass data assimilating evolution is closer to the 'true ocean' response than the free one.

The evolutions of the phytoplankton relative errors in the upper 0-20 m (not shown), in the lower 20-4000 m and in the all the water column show that the better increase of the assimilation error versus the free error is in the 0-20 outcome (November 2004). This increase is stepwise with oscillation around the 0.5 value, with approximately 50 % better error at the end of the seventy days. The increase of the phytoplankton in the bottom layer is also very good with final results of 0.6, slightly worse than the all column relative error (MFSTEP WP6-D5, November 2004).

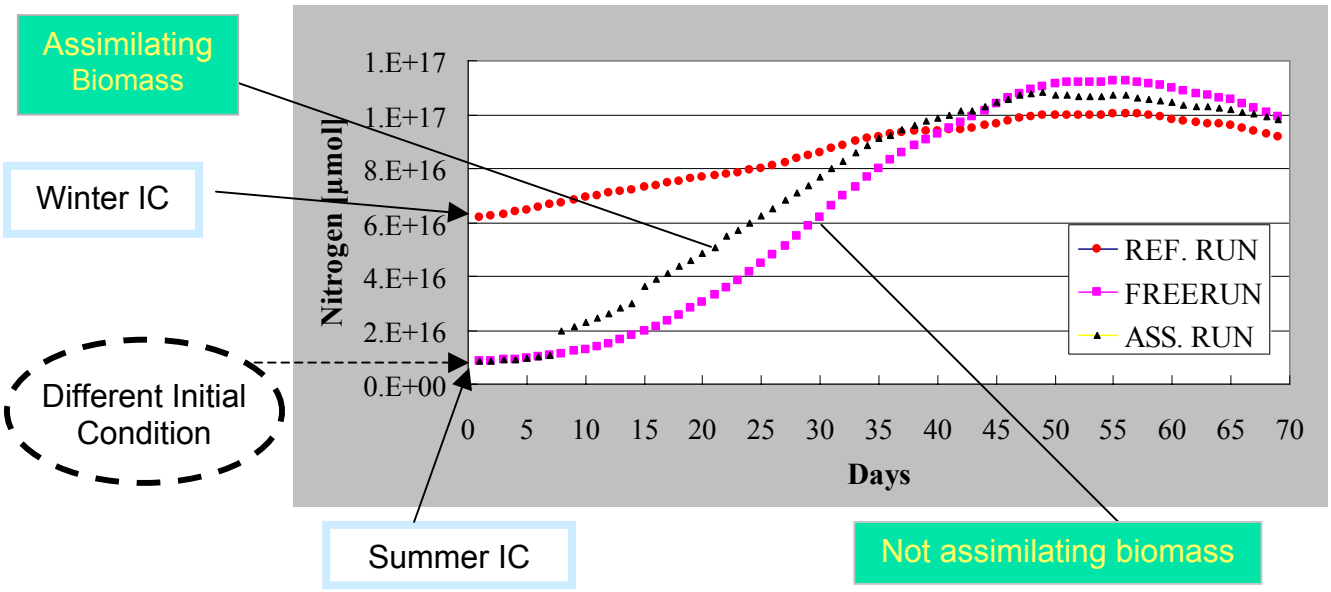

Figure 1.1. *Basin average phytoplankton (µmol N dm^{-3}) evolution for the three runs of the identical twin experiment. Red diamonds are the Reference Run averages, violet square the Free ones and black triangle the Assimilation ones.*

The discussion is deepening in the ITE overall reanalysis, between the observational strategy and plan, because in OSSEs for biomass an open problem is that total nitrogen, basin averaged and vertically integrated, requires several years to get close to the reference. This is connected to the fact that biomass is corrected by

assimilation only at surface layer and the dynamics cannot propagate the correction to the deeper layers when the water column is stratified during the summer periods. This is another motivation to move toward more sophisticated schemes in which correctly addressing at least bivariate assimilation of biomass and nutrient.

Moreover, the optimal assimilation in different seasons is going to be assessed quantifying the comparative results of winter experiment with summer modified biomass versus summer experiment with winter initial conditions. To this aim the SOFA system, after porting it on IBM SP5 AIX 5.2 512 Power 5 1.9 GHz CPU at CINECA, is used for performing Fraternal Twin Experiments (FTE) reported in the following of this WP6-D11 report.

2. Strategy of numerical experiments

After free evolution of about four years and four months, from the 1st September of 1998 to the 25th of December 2001*, the balanced NPZD model serves as testbed of fraternal twin experiments.

The numerical tests start after dynamical adjustment of the initial summer concentrations of phytoplankton and the other biochemical variables.

The forcing functions are ECMWF six hour forcing of the year 1998, considered as perpetual repeating year. The winter bloom period is here analyzed as case study representing the highly variability of the system and its reaction to different data coverages, see Fig. 2.1. Moreover, summer twin experiments are performed to understand how biochemical concentrations are affected by the stratified vertical structure of the water column, Fig. 2.2.

* The year depends on the length of the simulation from the 1/9/1998 beginning date; it marks only the adjustment duration and the evolution of the biochemical variables without any reference to the physics which maintains always its repeating cycle.

In the winter experiment three cases are investigated, namely the whole Mediterranean basin coverage, and the western and the eastern ones. In the first case the chlorophyll data are assimilated all over the basin from surface down to 20 m depth; in the second and the third cases assimilation is switched on in the specific basin, dividing the Sicily Channel at 13.5° E. In this way it should be possible to determine the relative efficiency, calculating the relative errors of the optimally interpolated versus the free run, when assimilating external chlorophyll in the western or in the eastern basin.

After free evolution of three years and four months, starting from experimental summer initial conditions injected at the beginning of September, the winter FTE span 84 days and comprise the free run and the assimilation runs. The runs begin from the final state of the numerical adjustment changing the winter pre-conditioning phytoplankton, which is substituted by the biomass field relative to the 25th of June; the three assimilation runs differ from the free run because of the assimilation through reduced-order optimal interpolation of the different coverage surface weekly averaged chlorophyll extracted from the control run. Their coverage is different as follows: all the Mediterranean basin, western basin only, eastern basin only.

On the other hand, the summer experiment provides an overall Mediterranean assimilation and consequently the effect is an integrated one; furthermore an analysis relative to the subbasin domain has been in this case carried out.

Being the chlorophyll a diagnostic model variable, same transformations have to be included in order to correct the phytoplankton variable.

There is a first stage in which the GCM interacts with SOFA where chlorophyll data are converted in phytoplankton ones by appling the chlorophyll to phytoplankton ratio (Chl/Phy)

$$XCORChl = K(d^{O} - (Chl/Phy)\, d^{m}) \qquad [2.1]$$

where XCORChl is the correction expressed in chlorophyll units, K is the Kalman filter, d^0 is the external datum, d^m is the model datum (phytoplankton in nitrogen units).

In the second stage SOFA interacts with GCM and the corrections in chlorophyll are transformed into biomass (nitrogen equivalent units).

XCORP=*Phy/Chl* XCORChl [2.2]

in which XCORP is the final biomass correction that completes the assimilation process at the current grid position.

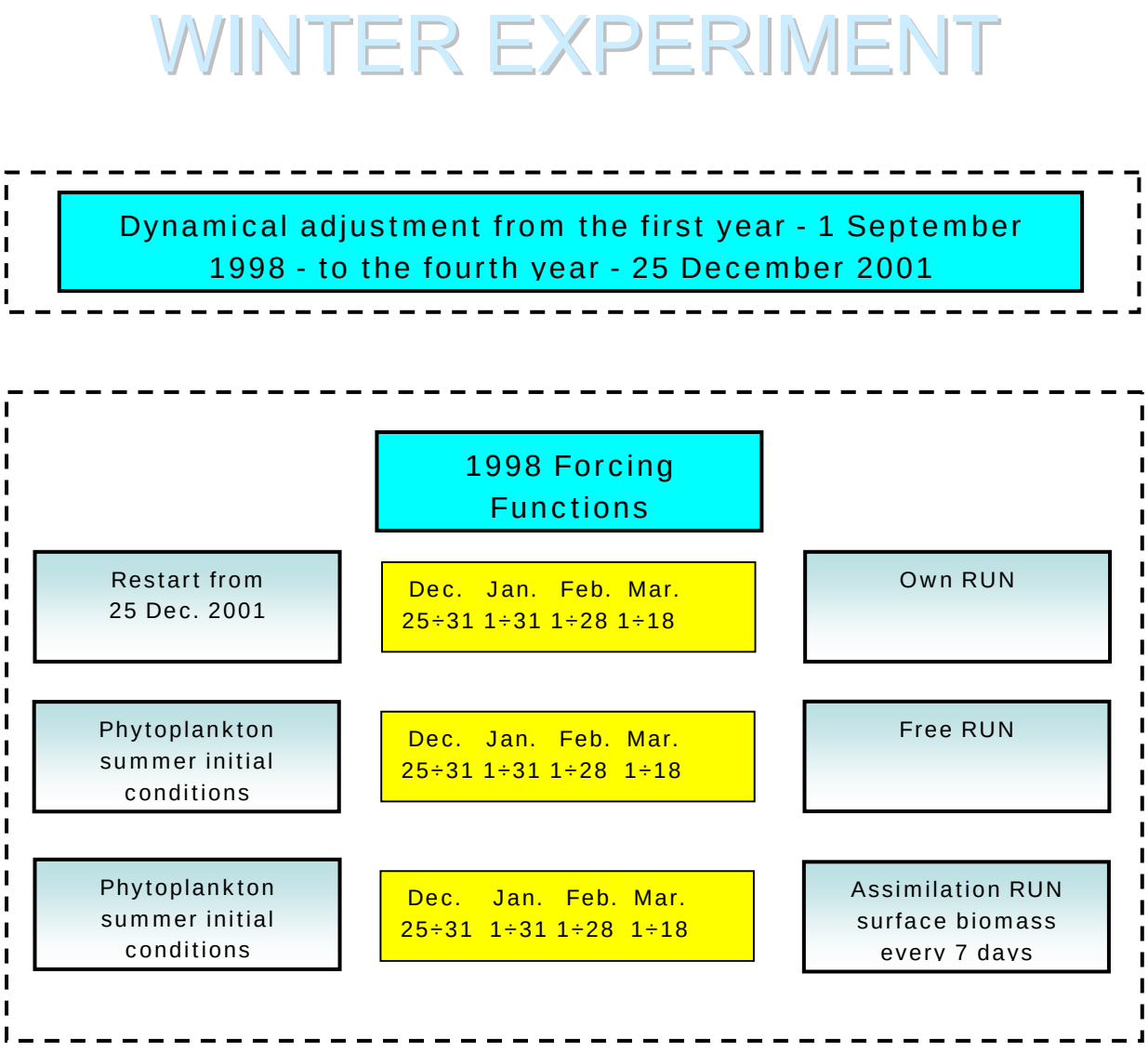

Figure 2.1. *Schematics of the winter fraternal twin experiments. The summer wrong initial conditions in the free and assimilation runs are the June 25 phytoplankton concentration maps. The other initial conditions are kept fixed.*

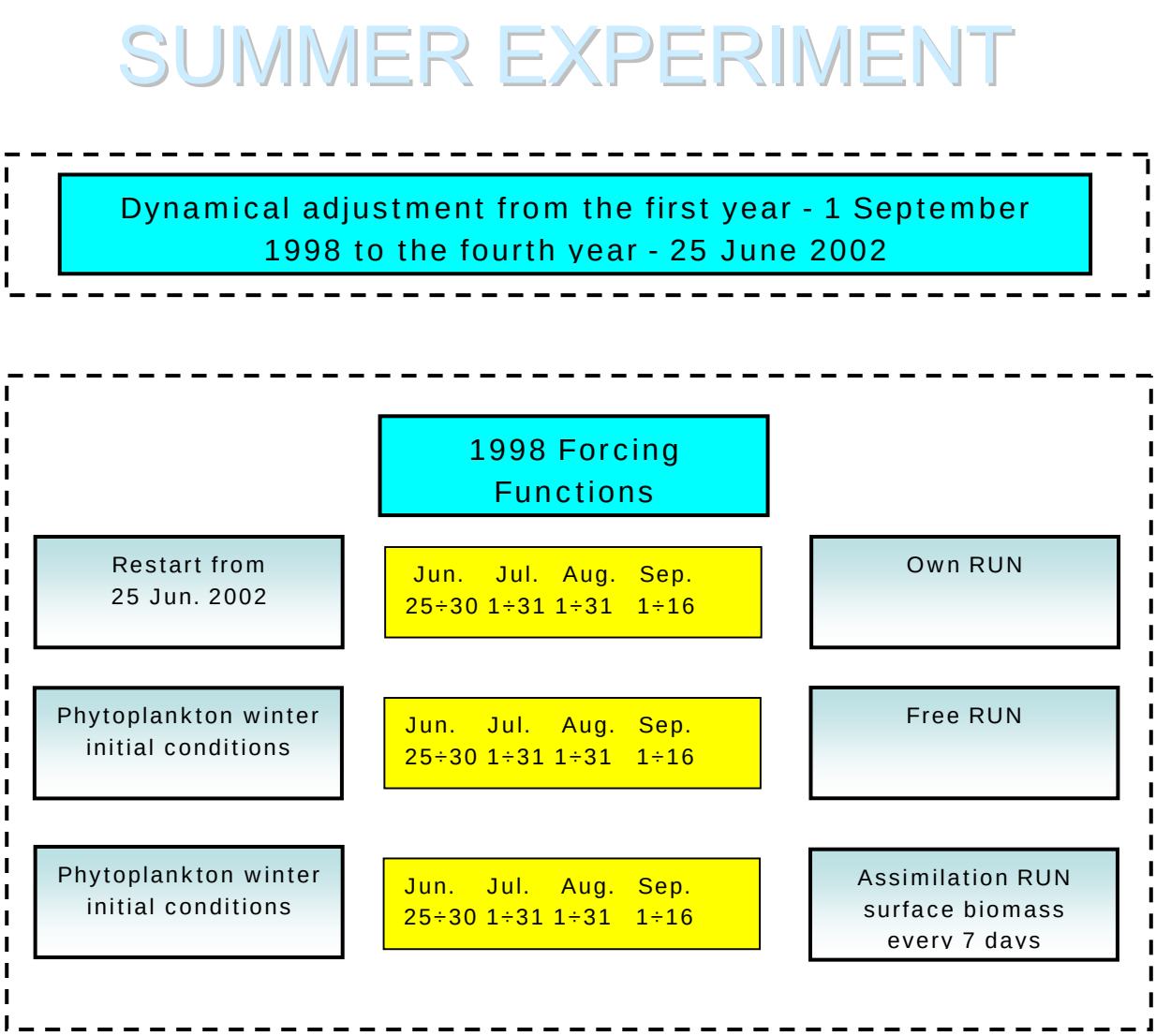

Figure 2.2. *Schematics of the summer fraternal twin experiments. The winter wrong initial conditions in the free and assimilation runs are the December 25 phytoplankton concentration maps. All the other initial conditions are kept fixed.*

The SOFA↔MOM data flow, occurring only when assimilation is switched on, is reported in Figure 2.3.

At the beginning of the run the vertical profiles are read by the module indat0VP, in /srcsofa/io/stdio. It reads 16083 weekly chlorophyll profiles one for each grid point; each profile is made of two data, the first for the upper 10 m level and the second for the adjacent subsurficial 10 m level.

After this input, VPput, in /srcsofa/lib, performs preprocessing of MVS format, packed Multivariate Vertical Sequence, at each gridpoint and every week, and records it in the SOFA database.

When the system needs the stored vertical profiles, it calls the module VPget searching vertical profiles records in SOFA database in line with the windowing cycle and storing their data unit pointers for current three-dimensional analysis.

After control is performed by module GetMvs in /scrmom, giving number of vertical data number for each model gridpoint number of interest, NMVS, and vector containing the indices of data for that gridpoint. The first represents the length of reduced MVS at gridpoint; the second is the reduced MVS vector at each gridpoint.

Module getCor in /srcsofa/gak/rooi4d gets computed corrections xcor(nmvs) in packed MVS form at gridpoint j. This program is called by the model at each gridpoint as a step in its reinitialization after each assimilation step.

At the end, and this completes assimilation cycle, module CORREC, in /srcmom, computes correction to model state using SOFA input.

In this framework the index inside the packed multivariate vertical sequence is made with the variable var_vs pointing to the number n_v of the tracer; and with the variable se_vs entering in the calculation of the kc level. The pointing to biomass, in the univariate correction operation of the system, is obtained introducing thirtyone values of the variable var_vs equal to four; in fact, phytoplankton is the fourth variable of the six tracers in the model, after temperature (first), salinity (second) and inorganic nitrogen (third). Moreover, the se_vs variable controls the 31 vertical level indices in the NPZD model. In particular, in this application only the first level and the second one are assimilated, so the characteristic index is 1 (one) for the surface chlorophyll datum and 2 (two) for the subsurface one.

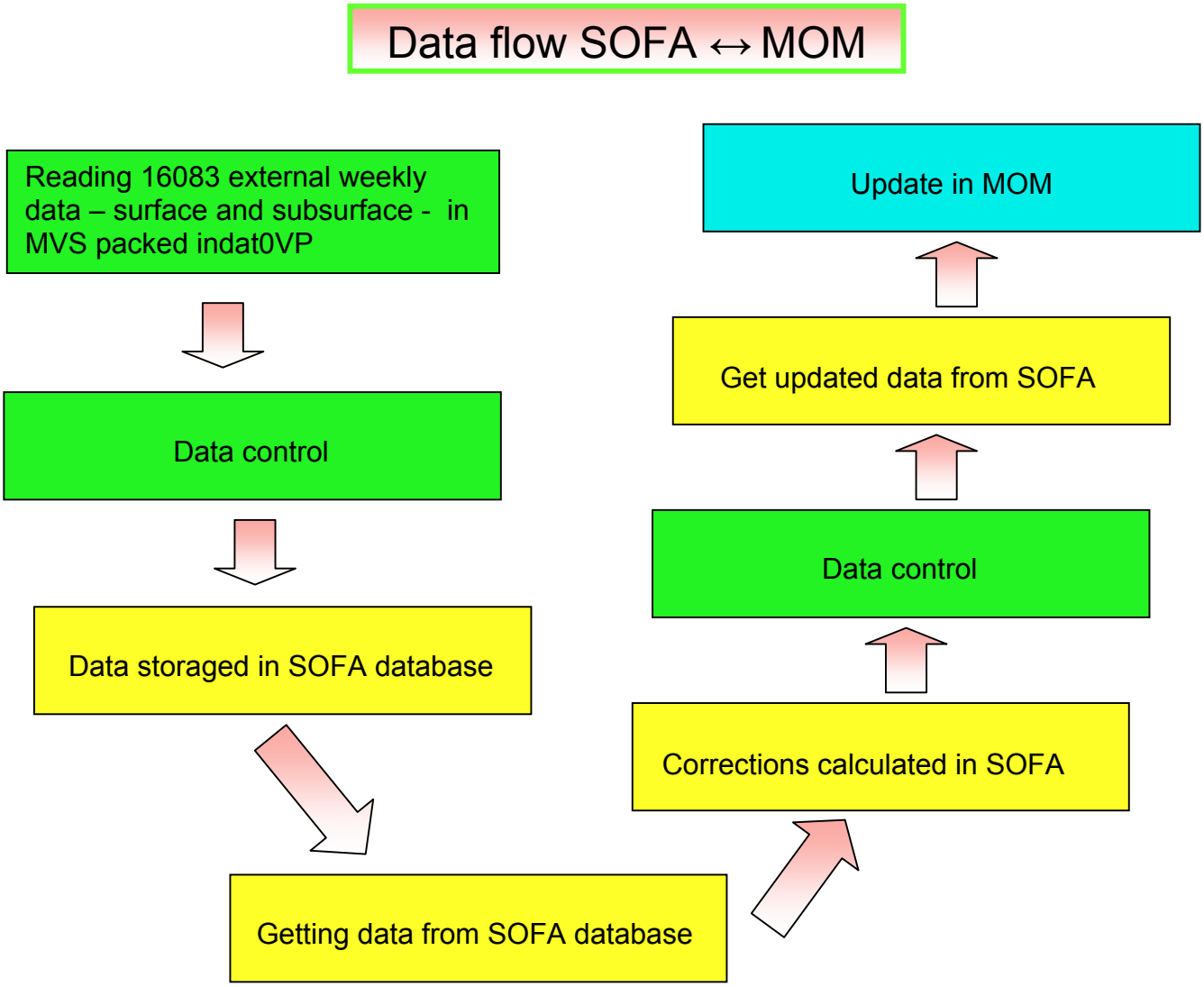

Figure 2.3. *External data flow and storage in SOFA database, statistical calculation and update in MOM.*

Relative errors and sensitivity analysis

The effects of assimilation upon the wrong phytoplankton initialized run and the efficiency along the 84 days are deduced from the relative error calculation. This is based on the assimilated to free sigma ratio, more exactly squared difference

between assimilated and control data divided by squared difference between free and control data.

$$\sigma = \frac{\sigma_{AC}}{\sigma_{FC}} = \sqrt{\frac{\frac{\sum_i (A_i - C_i)^2 \cdot Vol_i}{\sum_i Vol_i}}{\frac{\sum_i (F_i - C_i)^2 \cdot Vol_i}{\sum_i Vol_i}}} \qquad [2.3]$$

In equation 2.3 A_i, F_i, C_i are, respectively, the assimilated, free and control state variables (C is the control run at 1/4°) while vol_i are the cell volumes.

The problem consists in the fact that the ecomodel results are daily, while the control ones are monthly, and that the two horizontal grids differ, 1/8° versus 1/4°. The vertical levels are instead the same.

A linear time interpolation is applied in order to obtain 84 days of evolution, while the sigma spatial calculation is overcome by averaging the four contents at 1/8° inside each cell at 1/4°.

3. Chlorophyll inputs to SOFA

Synthetic chlorophyll data

Biomass surface data assimilation in the NPZD ecomodel is performed using the chlorophyll monthly assimilation maps in the pelagic Mediterranean Sea, as estimated through the simulations obtained with the three-dimensional ECHYM ecohydrodynamical model and its code at one quarter degree executed on SGI ORIGIN using the delivered FORTRAN code (Crise et al., 2003).

ECHYM biological submodel includes phosphorus and nitrogen cycles with two size-fractionated phytoplankton classes, zooplankton functional group and variable P:N:C ratio detritus. The simulations started from realistic phosphate and nitrate initial conditions injected in the ecomodel after spin-up of the hydrodynamics spanning four years simulation. The data file gave the monthly averages of the surface chlorophyll of the analysis of experimental data from the eighth, the ninth and the tenth years of the simulation of overall, physics plus biogeochemical evolution. This run considered marginal seas parameterization, river discharges and external atmospheric input in terms both of phosphate and of nitrate at surface.

ECHYM chlorophyll concentrations showed their highest values during early winter (December-February) in the western basin, while they tended to decrease in summer. In the Eastern Mediterranean the maxima were present in February and minima during summer. The correlation between the measured (1978-1985 CZCS maps) and the simulated data were quite good in the Western Mediterranean, around 0.86; it remained high also in the eastern basin, with 0.76. The biomass subbasin averages showed that the Western and Eastern Mediterranean exhibit similar response maintaining nearly unaltered the primary productivity of large cells in both basins, while that of small cells increased when including atmospheric input effects. Net primary production became 134.1 g C m^{-2} yr^{-1} (from 122.2 without atmospheric input) in the western basin; in the eastern basin the increase was higher up to 80.8 g C m^{-2} yr^{-1} (no atmospheric inputs value 59.2). The secondary production appeared less dependent on the atmospheric inputs, due to small cells driving of the primary production, with more efficient recycling of nutrients through the fast remineralization processes. These ECHYM results driven by high atmospheric inputs (Guerzoni et al., 1998) showed that the Eastern Mediterranean is typically dominated by small cells, this was seen in the no atmospheric input run, and also that the external nutrients supply contributes to ultraplankton bloom, this was understood in the atmospheric inputs run.

Chlorophyll equivalent

The ecosystem model is based on biomass expressed in nitrogen units. The ratio inside the plankton is taken fix and equal to the Redfield ratio 1:16:106:138. The conversion of units into chlorophyll requires the knowledge of the carbon constituting the cell with respect to the chlorophyll inside the cell. This type of conversion can be either statistical or dynamical. In the latter case the chlorophyll content and the biomass are both variables in terms of the evolution of the system and of the other biochemical variables; in the former case an analysis is done in terms of cells cultures and the statistical result is used to fix these two quantities.

In the following, surface chlorophyll, from surface till 20 m, is achieved by applying the statistical expression as obtained by Cloern *et al.* (1995) studying mainly diatom cultures. This expression is a function of temperature, irradiance at surface, and nitrogen availability:

$$\frac{Chl}{Phy} = 0.003 + 0.0154 e^{0.05T} e^{-0.059 \frac{I_0\left(1-e^{-K_z z_0}\right)}{K_z z_0}} \frac{N}{N + k_N} \qquad [3.1]$$

In equation [3.1] *Chl* and *Phy* are respectively the chlorophyll (mg Chl m^{-3}) and biomass concentrations (mg C m^{-3}). The conversion of the phytoplankton variable-*P*, from its nitrogen units in NPZD, to biomass variable-*Phy*, expressed in g of carbon, is made multiplying the former variable times the Redfield ratio, 106/16, and times the atomic weight, 12, of carbon. T is the potential temperature (°C) as given by the hydrodynamical model, the term k_z is the light extinction coefficient, in cm^{-1}, constant in our simulation and equal to $3.4 \cdot 10^{-4}$, and z_0 is the 20 m upper layer. The last term in equation [3.1] takes account for nutrient availability, inorganic nitrogen-*N* in this work.

Temperature, inorganic nitrogen and phytoplankton values are averaged between first (5m) and second (15m) model vertical level and then introduced in equation [3.1].

I_0 stands for superficial irradiance, expressed in langley day^{-1}, it has been calculated from 365 daily values according to Sverdrup *et al.* (1942) from the following Table 3.1.

Table 3.1. *Average amounts of radiation from sun and sky (After Kimball 1929). Units are expressed in gcal cm^{-2} min^{-1}. These data take into account the cloud coverage.*

Position	**Jan**	**Feb**	**Mar**	**Apr**	**May**	**Jun**	**Jul**	**Aug**	**Sep**	**Oct**	**Nov**	**Dec**
42°N - 66:70°W	0.094	0.138	0.212	0.272	0.306	0.329	0.302	0.267	0.230	0.174	0.115	0.086
42°N - 124°W	0.100	0.151	0.210	0.286	0.331	0.360	0.320	0.274	0.231	0.174	0.113	0.092
30°N - 65:77°W	0.146	0.165	0.238	0.285	0.317	0.310	0.301	0.282	0.239	0.188	0.169	0.142
30°N – 128:130°E	0.141	0.153	0.199	0.241	0.258	0.238	0.256	0.260	0.219	0.178	0.153	0.135

These data are converted into Langley per day (ly day^{-1}) with the trasformation gcal cm^{-2} min^{-1} * 4.18/60/(1e-4)/0.4845.

Also the photoperiod (P(t), with t as julian day) has been included, taking into account the effective day length and then distinguishing from bright and dark hours:

$$P(t)=0.5-0.125*\cos((2\pi*(t+10))/365). \qquad [3.2]$$

We have built the optimized formulation for the superficial irradiance; the target is a best fit between the data in Table 3.1 and the following irradiance expression:

$$I_{sup}(t) = P(t)\left[A - B\cos\left(\frac{2\pi(day+10)}{365}\right)\right] \qquad [3.3]$$

After the optimization, the A and B parameters are *A*=607. and *B*=126.

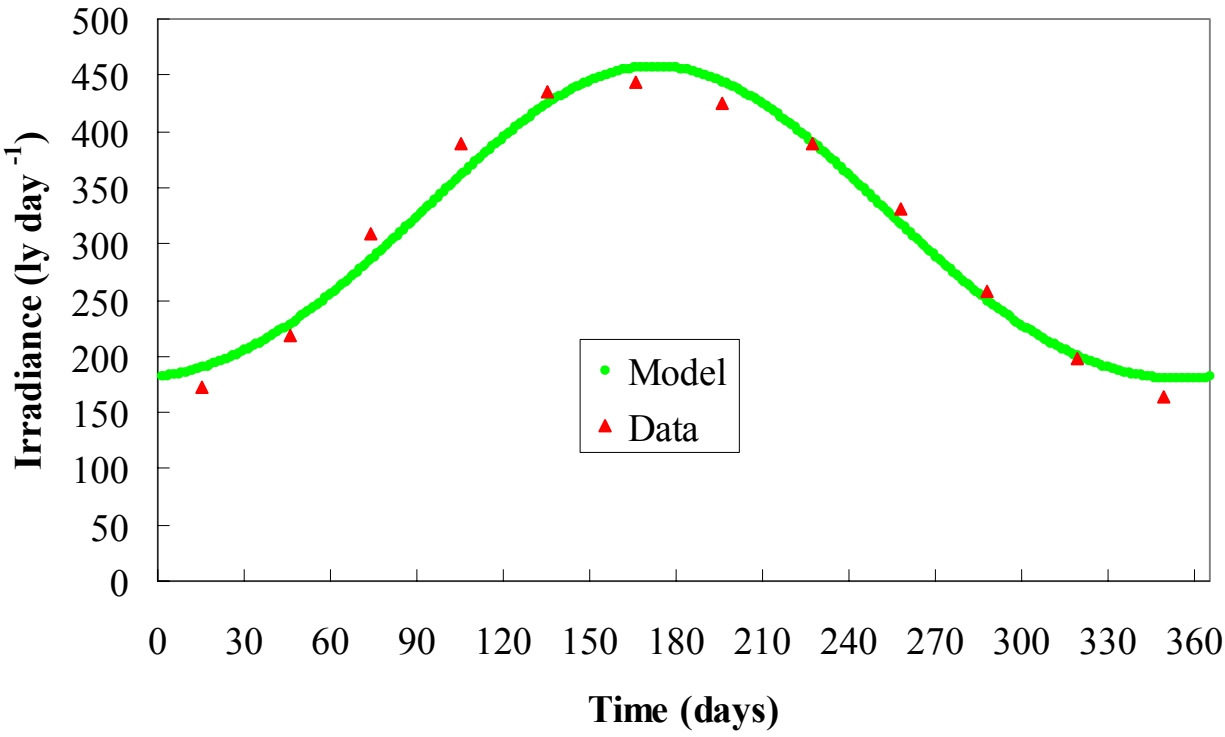

Figure 3.1. *Optimized* I_{sup} *irradiance formulation introducing the photoperiod (green line) with monthly averaged data (red triangles from Sverdrup et al. (1942)). The resulting line reported in Figure has an error of 16. ly day*$^{-1}$.

These parameters are introduced in the final I_0 expression, with the reflected and long wave radiation:

$$I_0(t) = P(t)(1-ref)(1-lw)\left[607. - 126.\cos\left(\frac{2\pi(day+10)}{365}\right)\right] \qquad [3.4]$$

which is converted from ly day^{-1} to mol quanta day^{-1} m^{-2} in order to be applied in equation [3.1], using the conversion ly day^{-1} * 0.4845 * 0.015 * 24. Here *ref* , equal to 0.15, stands for reflected light fraction and *lw* , equal to 0.55, means long wave radiation fraction.

Space and time interpolation

Chlorophyll data are spatially interpolated starting from monthly superficial (0-20 m) ECHYM (ADIOS, 2003) evaluations. There are 2 matrices with 3 indices: longitude, latitude and time. C1/4 is the ECHYM matrix with grid resolution at 1/4 degree, 182x57x12 knots, and C1/8 is the matrix that we have to build according to SOFA resolution at 1/8 degree, 363x113x84 knots.

The first step consists in defining C1/4 and C1/8 common grid points, that is to say C1/4(1,1,t)=C1/8(1,1,t), C1/4(2,1,t)= C1/8(3,1,t), C1/4(3,1,t)= C1/8(5,1,t); because the resolution is 1/4 degree in C1/4 and 1/8 degree in C1/8. At this stage, Fig. 3.2, the new C1/8 matrix structure appears as follows:

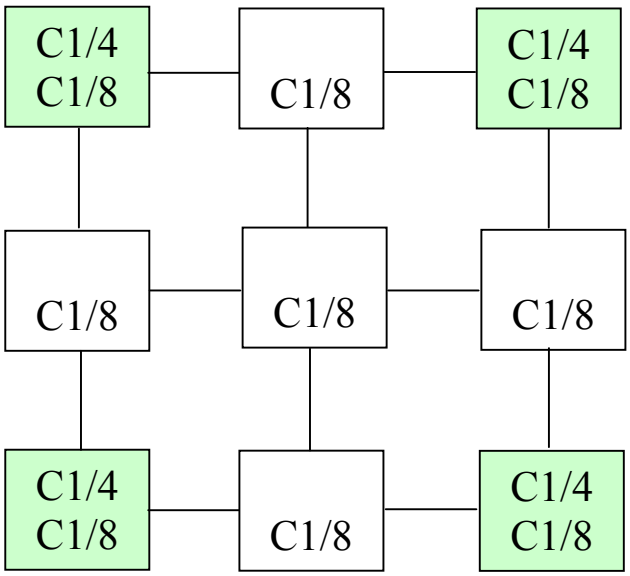

Figure 3.2. *Scheme representing the knots at 1/4° and 1/8° grid resolution. The green knots are in common.*

The next step provides D1, D2, D3, D4 grid points; it is based on the averaged value between two adjacent data in C1/4 matrix both in X and Y directions; for example D1 is the average between the 2 red boxes in Fig. 3.3. If a null averaged value is detected then D1 will be equal to zero.

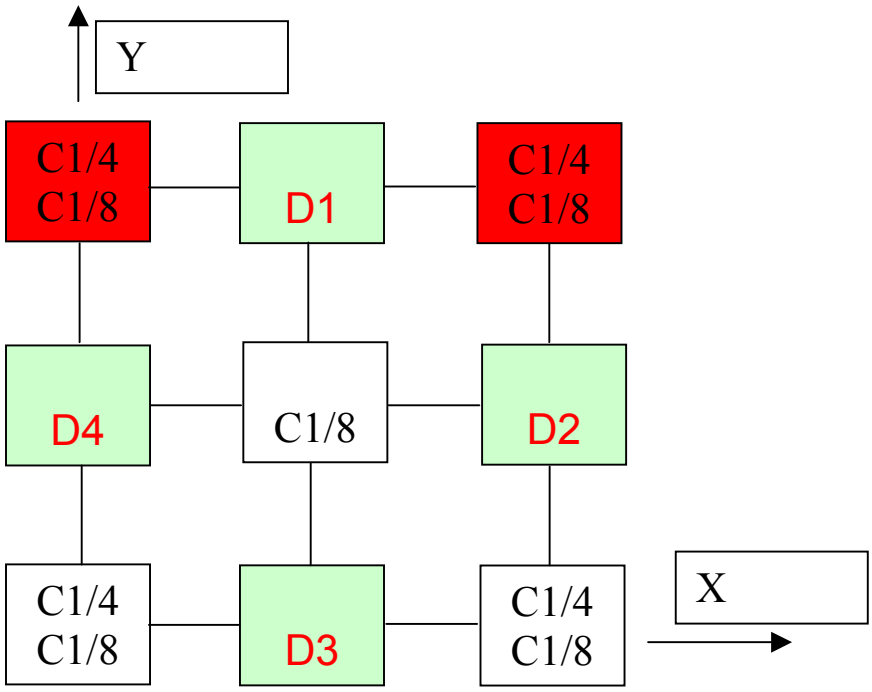

Figure 3.3. *Scheme representing the knots at 1/4° and 1/8° grid resolution. The two red knots determine D1.*

In the Fig. 3.4 the program provides C1/8 in the center.

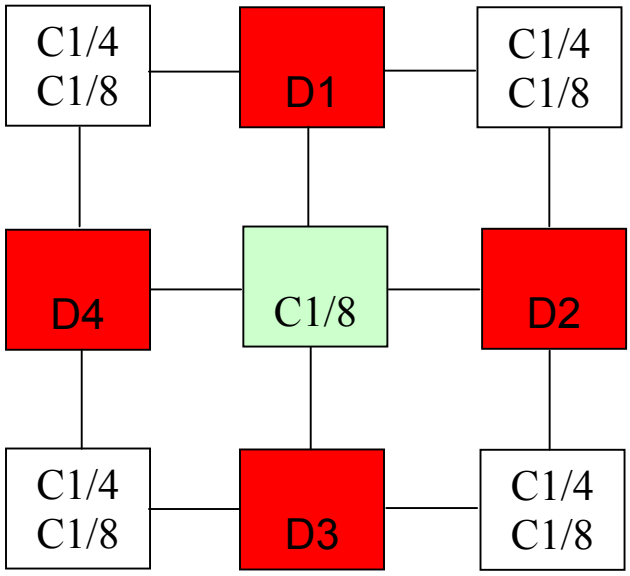

Figure 3.4. *Scheme representing the knots at 1/4° and 1/8° grid resolution. The four red knots determine the central green datum at 1/8°.*

The calculation is based on averaging the D1, D2, D3, D4 values, if they are null then the central datum will be zero.

At this stage the 1/8 degree structure is completed, however the sea grid points in SOFA are not automatically the same in matrix C1/8. The problem now consists in overcoming this sea grid misleading and then if SOFA expects a sea point while C1/8 not, a new vector is defined with 8 adjacent points, evidenced in Fig. 3.5, if the averaged value is null then a scansion to the next nearer datum is performed in the X and Y directions.

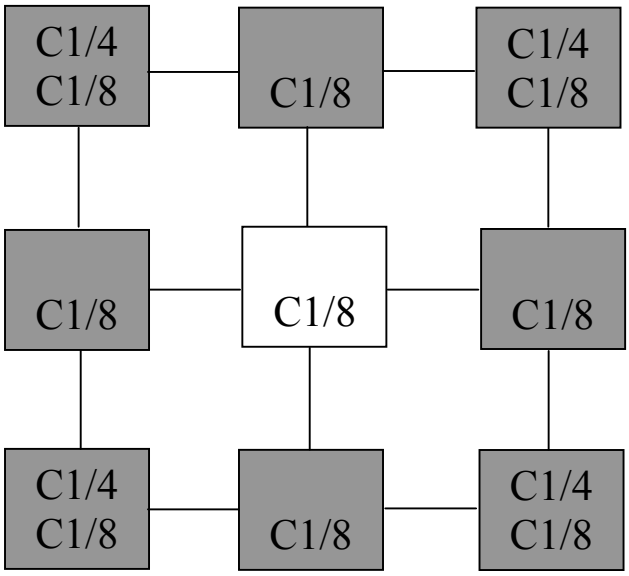

Figure 3.5. *Scheme representing the knots at 1/4° and 1/8° grid resolution. The eight knots determine the central datum at 1/8°.*

Particularly the program tries firstly forward along X (where possible, Fig.3.6), the length interval derives from multiple tests. In some cases 2 points are required to overcome the problem but in other ones 4 points are needed and then a general length is adopted.

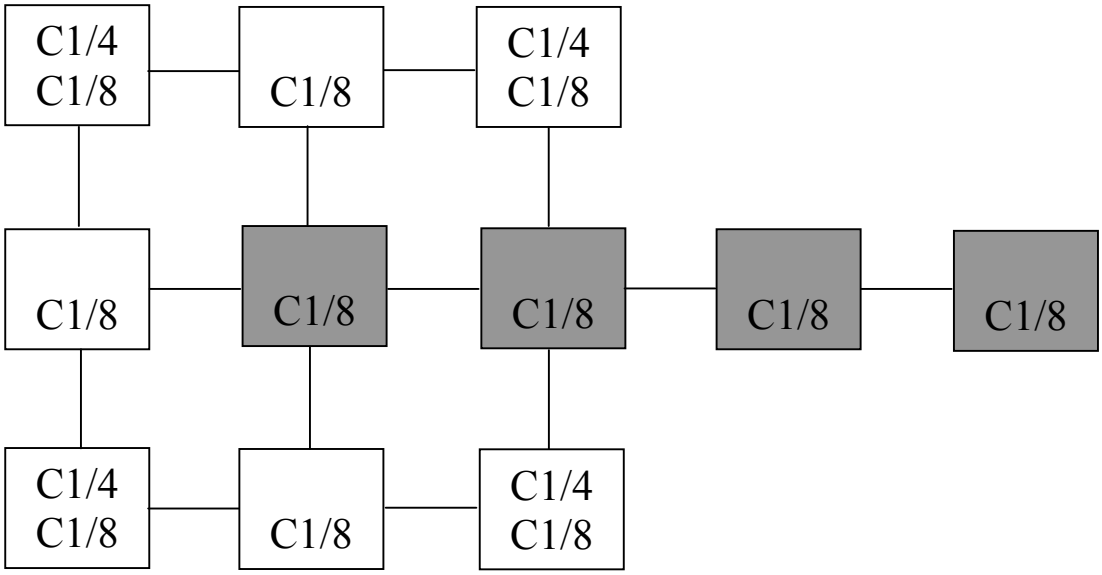

Figure 3.6. *Scheme representing the knots at 1/4° and 1/8° grid resolution. A forward scansion along the X axis is shown.*

if there is no value, it tries backward along X (where possible, Fig. 3.7)

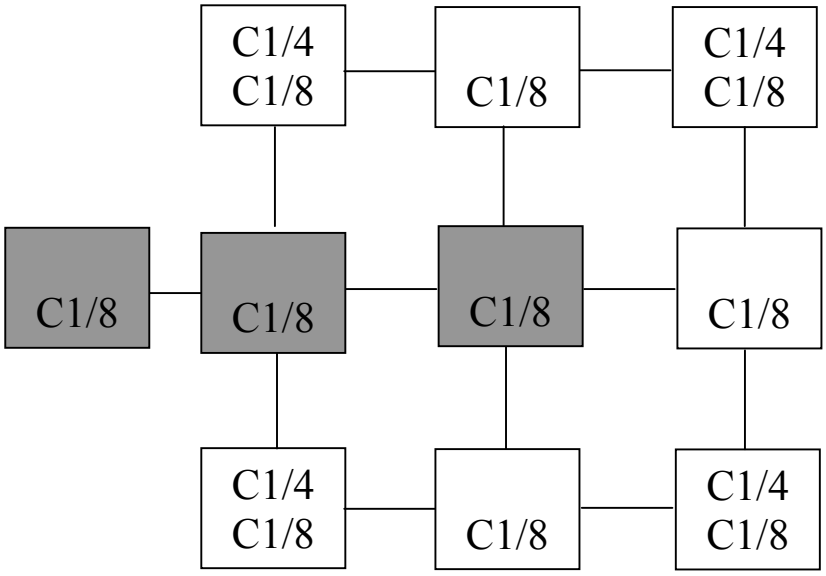

Figure 3.7. *Scheme representing the knots at 1/4° and 1/8° grid resolution. A backward scansion along the X axis is shown.*

if there is no value, it tries upward along Y (where possible, Fig. 3.8)

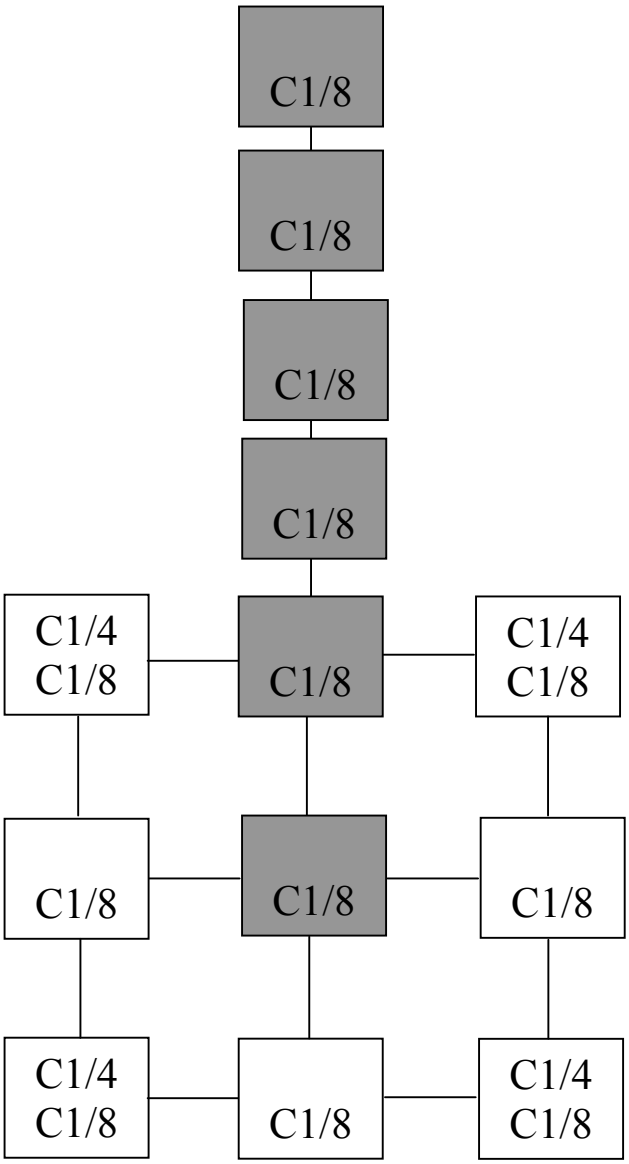

Figure 3.8. *Scheme representing the knots at 1/4° and 1/8° grid resolution. A upward scansion along the Y axis is shown.*

if there is no value, it tries downward along Y (where possible, Fig 3.9)

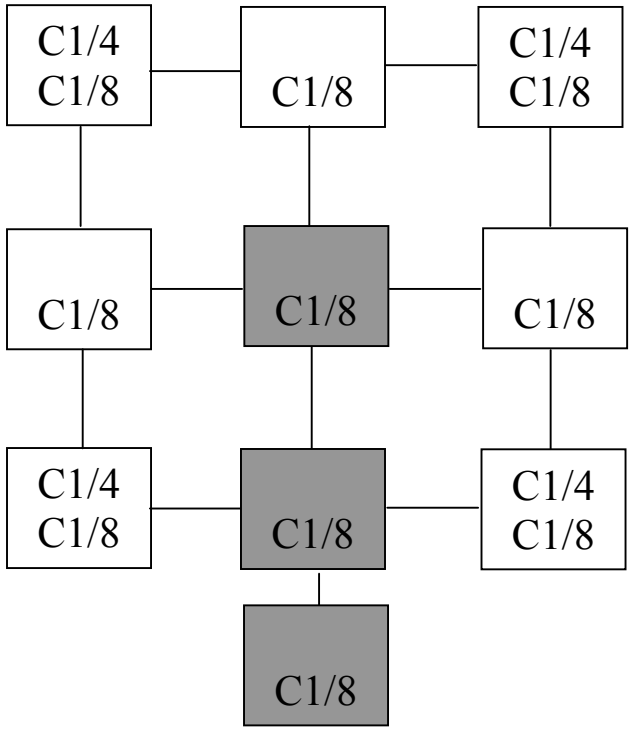

Figure 3.9. *Scheme representing the knots at 1/4° and 1/8° grid resolution. A downward scansion along the Y axis is shown.*

and finally since there are two cases, it operates diagonally (Fig. 3.10).

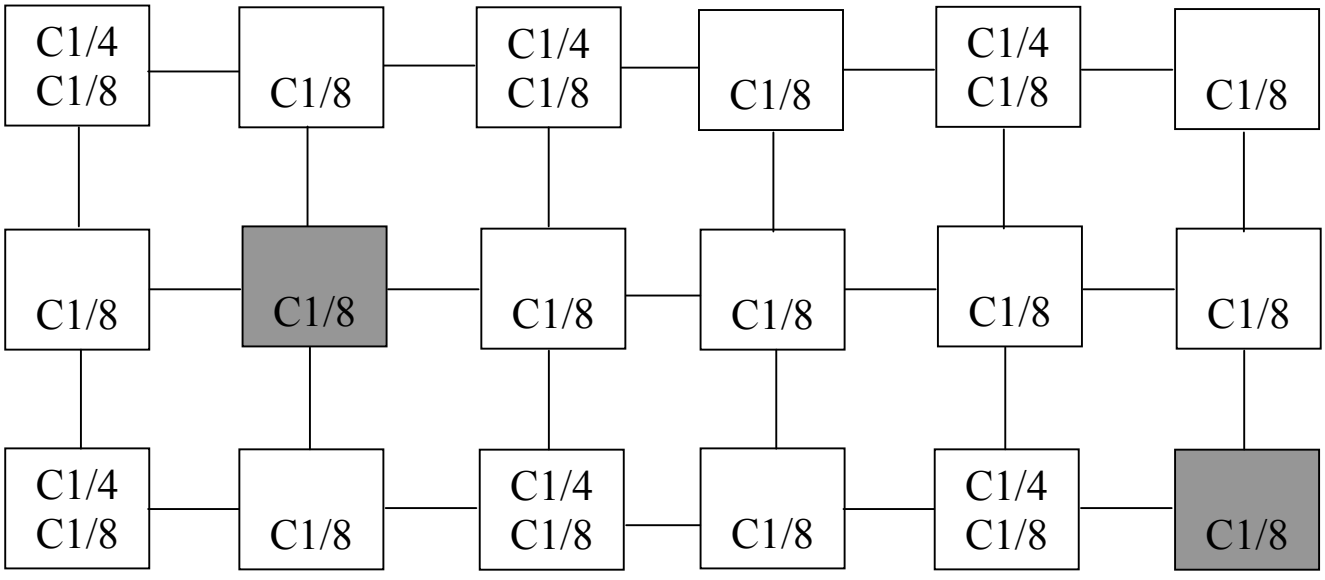

Figure 3.10. *Scheme representing the knots at 1/4° and 1/8° grid resolution. A particular scheme of resolution is adopted.*

At this stage C1/8 is spatially compatible with SOFA sea grid points, next step provides temporal interpolation, because C1/4 matrix is monthly averaged (12 months) and C1/8 needs some specific days data for assimilating weekly biomass. Each monthly value is associated to the 15th day of the month and then linearly interpolated. In the summer assimilation experiment the starting day is the 2nd of July and the last day is the 16th of September. The interpolation on the 2nd and the 9th of July is performed considering June and July; that on 16, 23, 30 July and 6 and 13 August, considering July and August; that on 20, 27 August and 3, 10, 17 September, considering August and September.

These interpolated values will be inserted into each weekly file, for each grid point in the first 2 vertical levels. Their content consists in an initial row with standard error equal to 0.07, a data unit identifier, the longitude and the latitude, the day number (7 for the first cycle, 14 in the second one, ecc.), the number of vertical levels (2), the corresponding levels (1 and 2, that is 5m and 15m), the biomass data. The initial longitude is 6°W (without Gibraltar Strait), and also the North Adriatic and North Aegean Sea are excluded from the assimilation domain.
In Fig. 3.11 the basin averaged chlorophyll content is represented during the year both for ECHYM and interpolated grid. The best situation falls in November where C1/8 is 0.012% greater than C1/4. On the other hand, the worse situation falls in January where C1/8 is 3.135% lower than C1/4.

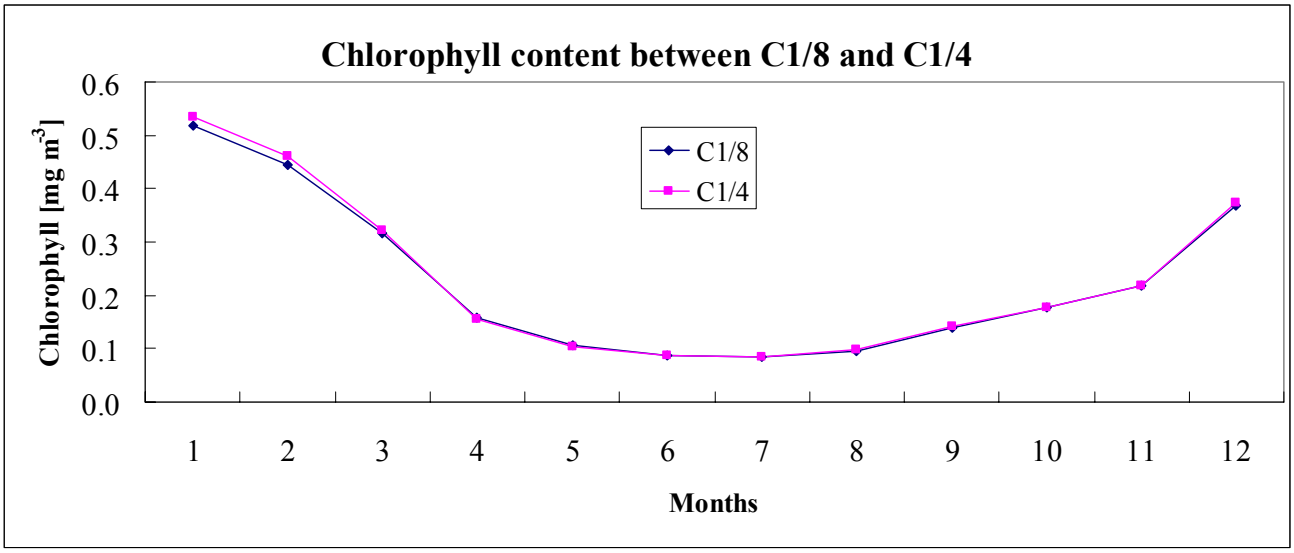

Figure 3.11. *Comparison between 1/4 ° (C1/4) and interpolated chlorophyll (C1/8).*

4. Biogeochemical model developments

Study of the Mediterranean ecosystem is complex because of the superposition of different effects. In part this is common to the World Ocean and in part is specific. The origin of this problem comes from the varieties of physical processes that are present in the basin with a lot of consequent outcomes at the level of the geochemistry, of the life inside the sea, and of the ecology.

The points to be addressed in any synthetical approach are the following. In this sea there is no permanent thermocline and the interpretation must consider the seasonal thermocline influence. The residence of the deep water masses is with relatively short residence times. The low tides induce selected friction along the shelf areas. This temperate basin has large interannual variability. There is a strong coupling shelf-open sea.

The physical part has as its counterpart the major fact that the Mediterranean has no major exchanges, except the three following enumerated in order of minor importance: the inflow of freshwater by the main rivers and by the Bosphorus Strait, prevalently affecting coastal areas; the atmospheric inputs in term of matter, which modify the higher layer concentrations in terms of the different oligoelements and the composition of the water masses; the inflow/outflow with the Atlantic Ocean, influencing the conveyor belt.

These three facts determine: an oligotrophic ecosystem, a deep benthic system that cycles at low energy sill, light intensity different in a zonal pattern, anomalous nutrient ratio with respect with Redfield et al. (1963) one in the World Ocean.

This work recognizes these interconnecting parts of the mechanisms and addresses the development of micro-elements in the monitoring system for the Mediterranean ecosystem, in particular towards evaluation of trends and budgets, considering that the evolution of variabilities of the chemical and biological characteristics of the Mediterranean marine ecosystem requires an integrated approach.

The aim of simulating relevant biological processes of the nitrogen cycle has led to the development of coupled basin-scale general circulation ecomodels of the Mediterranean Sea (Crispi et al., 1998). One could argue whether these models really simulate ecosystems or should rather be named biogeochemical models. That is, because such models simply transfer mass from an inorganic reservoir into organic pools and may lack, for instance, important ecological processes. Nevertheless, the terminology ecosystem model is commonly used for those biological models that include parameterisations mostly describing mass exchange rates. In general the model parameters are considered to be constant in time. Hence, the model solutions strongly depend on the choice of the corresponding biological parameters which, in addition, need to represent a diversity of individual organisms, grouped into compartments of, for example, phytoplankton and herbivorous zooplankton. Since

the model parameters should represent a complex system in such a simple way, their appropriate estimate remains a major challenge.

Primitive equation model

The dynamics of the Mediterranean oligotrophic ecosystem is studied through its coupling with the Mediterranean basin circulation as simulated by a general circulation model driven by high frequency forcing. This is the Geophysical Fluid Dynamics Laboratory Modular Ocean Model (Pacanowski et al., 1991). MOM is finite difference formulation of the primitive equations governing ocean circulation. These equations consist of the hydrostatic Navier-Stokes equations along with a nonlinear equation of state which couples the two active tracers, temperature and salinity, to the fluid velocity. The surface displacements in the ocean are relatively small compared to interface displacements between layers within the fluid, and rigid-lid approximation is used. Their affect on the solution is represented as a pressure against the rigid lid at the ocean surface. Eddy-viscosity is the basis for the form of the friction.

Thus the hydrodynamics are based on the following fully 3-D primitive equations in a spherical coordinate system *(λ, φ, z)*, where *λ* is longitude increasing eastward, *φ* is latitude increasing northward and *z* is positive upward with zero defined at the ocean surface:

$$\frac{\partial \bar{v}}{\partial t} + (\bar{u} \cdot \nabla)\bar{v} + \bar{f} \times \bar{v} = -\frac{1}{\rho_0}\nabla_H P - A_H \nabla_H^4 \bar{v} + A_V \frac{\partial^2 \bar{v}}{\partial z^2} \qquad [4.1]$$

$$\frac{\partial p}{\partial z} = -\rho g \qquad [4.2]$$

$$\nabla \cdot \bar{u} = 0 \qquad [4.3]$$

$$\frac{\partial T}{\partial t} + (\bar{u} \cdot \nabla)T = -K_H \nabla_H^4 T + K_V \frac{\partial^2 T}{\partial z^2} + \alpha_T (T - T^*) \qquad [4.4]$$

$$\frac{\partial S}{\partial t} + (\bar{u} \cdot \nabla) S = -K_H \nabla_H^4 S + K_V \frac{\partial^2 S}{\partial z^2} + \alpha_S (S - S^*) \qquad [4.5]$$

$$\rho = \rho(T, S, p) \qquad [4.6]$$

In the preceding equations $\bar{v} = (v_\lambda, v_\varphi)$ and $w = v_z$ are respectively the horizontal and vertical components of the velocity $\bar{u}$; T and S are the temperature and salinity, while p and ρ represent the pressure and density. The Coriolis parameter is given by $\bar{f} = 2\Omega \sin\varphi \bar{k}$ and g is the gravity constant. A_H and A_V are the horizontal and vertical constant eddy viscosity coefficients, while K_H and K_V are the horizontal and vertical constant turbulent diffusion coefficients. Equation [4.6] is the UNESCO equation of state for sea water. Equations [4.4] and [4.5] are the equations for the active tracers potential temperature and salinity. The second term in [4.1], [4.4] and [4.5] is the advection (differential) operator in spherical coordinates and includes the three velocity components and the radius of Earth.

In particular, the simulations reported here adopt a GCM for the Mediterranean Sea plus a buffer zone representing the Atlantic inflow/outflow. The transport through the Strait of Gibraltar is parameterized in an extended area, where temperature and salinity are relaxed towards annual climatological fields.
The biharmonic horizontal eddy viscosity is $0.5 \cdot 10^{18}$ cm^4 s^{-1} and the biharmonic horizontal eddy diffusivity is $1.5 \cdot 10^{18}$ cm^4 s^{-1} for physical tracers. The vertical viscosity is 1.5 cm^2 s^{-1}, the vertical diffusivity for temperature and salinity is 0.3 cm^2 s^{-1}.

The model is integrated throughout all the Mediterranean basin, with a horizontal spatial discretization of one eighth degree and with a vertical resolution of 31 levels. On the same grid the equations describing nitrogen uptake, and grazing and remineralization processes, are integrated. The vertical levels (layers) are unevenly spaced down to 4000 m, and the tracer values, temperature, salinity and biochemical ones, biomass among the others, are placed at 5, 15, 30, 50, 70, 90, 120, 160, 200,

240, 280, 320, 360, 400, 440, 480, 520, 580, 660, 775, 925, 1150, 1450, 1750, 2050, 2350, 2650, 2950, 3250, 3550, 3850 m.

A standard convective adjustment procedure is applied, mixing the contents of two adjacent levels, when static instability appears in the water column. When instabilities arise in the biogeochemistry, biological sources and sinks are set to zero.

The α terms in equations [4.4] and [4.5] are the Newtonian restoring terms which are different from zero only in selected regions of the model. Both for the physical and for the biogeochemical variables $\alpha_{T/S} = 1.0\ day^{-1}$.

Air-sea physical parameterizations account for the heat budget at the air-sea interface in the sense of Roussenov *et al.* (1995). The surface heat forcing is computed in an interactive way with 6-hourly European Center for Medium Range Weather Forecast – ECMWF atmospheric reanalysis fields and sea surface temperature from the model. The meteorological data used are the atmospheric temperature and humidity at 2m, wind components at 10m and the percentage of the cloud cover. In the simulations here reported, perpetual year simulation is attained with the forcing data of the 1998: after the 31st of December the year cycles with the 1st of January data of the 1998 dataset.

The specification of salt fluxes at the sea surface is generally related to the problem of prescribing precipitation-evaporation values, however the problem is solved by imposing the salinity structure at the first model level, as indicated by equation [4.5]. The surface salinity boundary condition is a relaxation to climatological monthly mean values.

Here in the Mediterranean MOM model the solid boundaries are non-slip and insulating for temperature and salinity. The bottom is free slip and insulating. The momentum flux through the sea surface comes from two sources - the wind stress and the heat transfer. 3-D hydrodynamics equations [4.1] – [4.6] with relevant boundary conditions are solved through a second order finite difference method on the numerical B-grid, U and T cells, with 31 vertical levels. The time step is 900 sec (15 min). The standard Fortran 77 is used for preparing the code. The programming

approach is modular and there are different additions and modifications to this model. Computers having C-language pre-compilers and running UNIX-based operating system are required to manage the MOM code because of the choice of compilation time options.

NPZD ecomodel

The biological variations in the ocean are relatively small and difficult to detect against high background values. For the determination of this variability, an NPZD ecosystem for the Mediterranean Sea has been set up starting from nitrogen units.

Firstly, a reciprocal interaction between the elemental composition of marine biota and their dissolved inorganic resources are assumed, whereby the nutrient elements are taken up and released in fixed proportions of C:N:P of 106:16:1. Secondly, it is assumed that the biological production in the ocean is principally limited by the availability of nitrogen, meaning that the supply of nitrogen also determines the amount of carbon incorporated into biomass. Production based on nitrate, which newly enters the euphotic zone, where light availability is sufficient for net growth, is referred to as new production and is differentiated from production based on the remineralized compounds of nitrogen. On average, the export flux of organic material from this upper oceanic layer equals the new production.

The 3-D coupling of the biological tracer with hydrodynamics and its parameterization are on the same grid of the Mediterranean circulation model, one eighth degree, where the equations describing nitrogen uptake, and grazing and remineralization processes, are integrated. Every variable has a positive flux to the following: the uptake from nitrate to phytoplankton; the grazing from phytoplankton to zooplankton; the mortality from zooplankton to detritus; and the remineralization from detritus to nitrate. Also the specific mortality and lysis from phytoplankton to detritus is taken into account. These five fundamental fluxes are completed by cross

fluxes from zooplankton to nitrate, the excretion, and from phytoplankton to detritus, the sloppy feeding (Fig. 4.1).

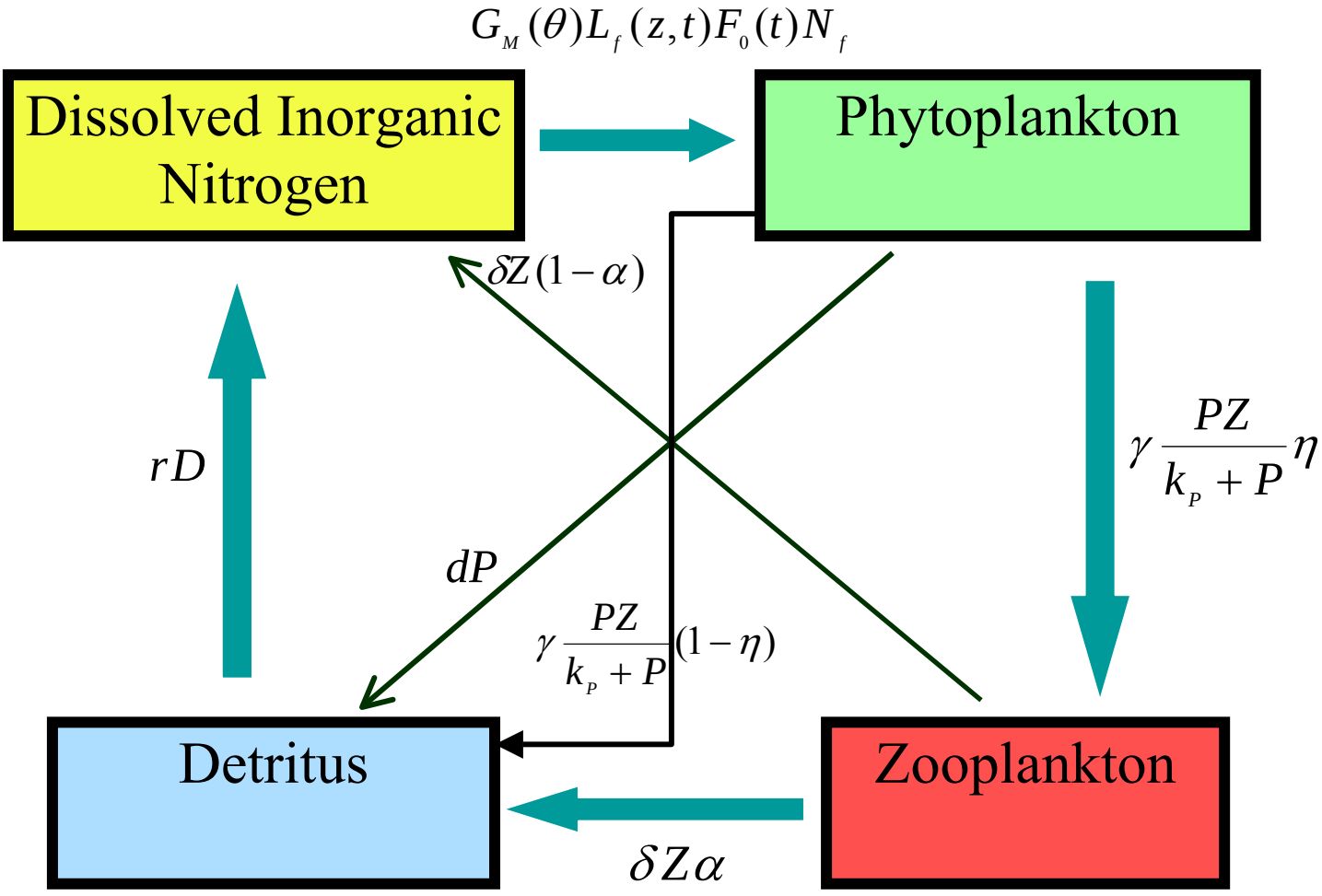

Figure 4.1. *NPZD model compartments with the relative quantitative fluxes. From left top: uptake, grazing, mortality, remineralization. In the cross arrows zooplankton excretion, from bottom right, and sloppy feeding and phytoplankton mortality from top right.*

All these terms are linear kinetics except for uptake. The latter is of the form

$$G_M(T)L_f(z,t)F_0(t)N_f \qquad [4.7]$$

G_M is the temperature dependent growth rate.

L_f is the light limitation function according with Steele factor (1962) given by

$$L_f(z,t) = \frac{I_0(t)e^{-k_z z}}{I_{opt}} e^{1-\frac{I_0(t)e^{-k_z z}}{I_{opt}}} \qquad [4.8]$$

$F_0(t)$ is the photoperiod, i. e. the irradiance day length (Carrada et al., 1983),

$$F_0(t) = 0.5 - 0.125\cos\left(\frac{2\pi(day+10)}{365}\right) \qquad [4.9]$$

Finally N_f is the Michaelis-Menten formulation for the limitation in terms of available inorganic nitrogen N, considered as sum of nitrate plus ammonia.

All the parameters are chosen in literature ranges for oligotrophic environments, Appendix 2.

Biochemical initial conditions

Initial phytoplankton is the average of the summer stations in Berland et al. (1988); zooplankton is initialized at one ninth of the phytoplankton value; detritus is set in the first 6 vertical levels, till 100 m depth, according to Coste et al. (1988).

Mean nitrate summer conditions for stations DH3, DS4, DJ7 (in correspondence to the stations by Berland et al. (1988)) are extracted from the on line climatology http://doga.ogs.trieste.it/medar/climatologies/medz.html (Manca et al., 2004).

Averaged values are interpolated the 31 vertical levels of the model. This final profile initializes nitrate variable for all the Mediterranean basin.

Restoration at Gibraltar, –5.5W westerly, is very close to field data for nitrate (Osborne et al., 1992), while it attains the basin initial profiles for phytoplankton, zooplankton and detritus. In addition, Adriatic (Zavatarelli et al., 1998) and Aegean (McGill, 1970) are restored to prescribed inorganic nitrogen values, respectively northerly 43°N and 38°N.

Terrestrial inputs are assigned on the basis of yearly average of nitrogen loads for the Gulf of Lions (Durrieu de Madron et al., 2001) and Nile delta (Hamza, 2001). These sources of nitrate are distributed in the area of the Rhone river mouth and in front of the Nile delta. No fresh water is added and dilution effects are taken into account through the surface climatological restoration of the salinity.

Atmospheric nitrate scheme

Atmospheric loads are summarized in the Figure 4.2 and follow the work of Guerzoni et al. (1999). Different depositions upon the western, the central and the eastern regions are considered. In the scheme are also reported the different run configurations: the reference run (RRUN) has been achieved without any inputs (either terrestrial or atmospheric), the inorganic input run (IRUN) takes account of the 100% input in the superficial nitrate compartment, finally the fractionated run (FRUN) divides the inputs between the inorganic nitrogen (50%) and detritus (50%) compartments.

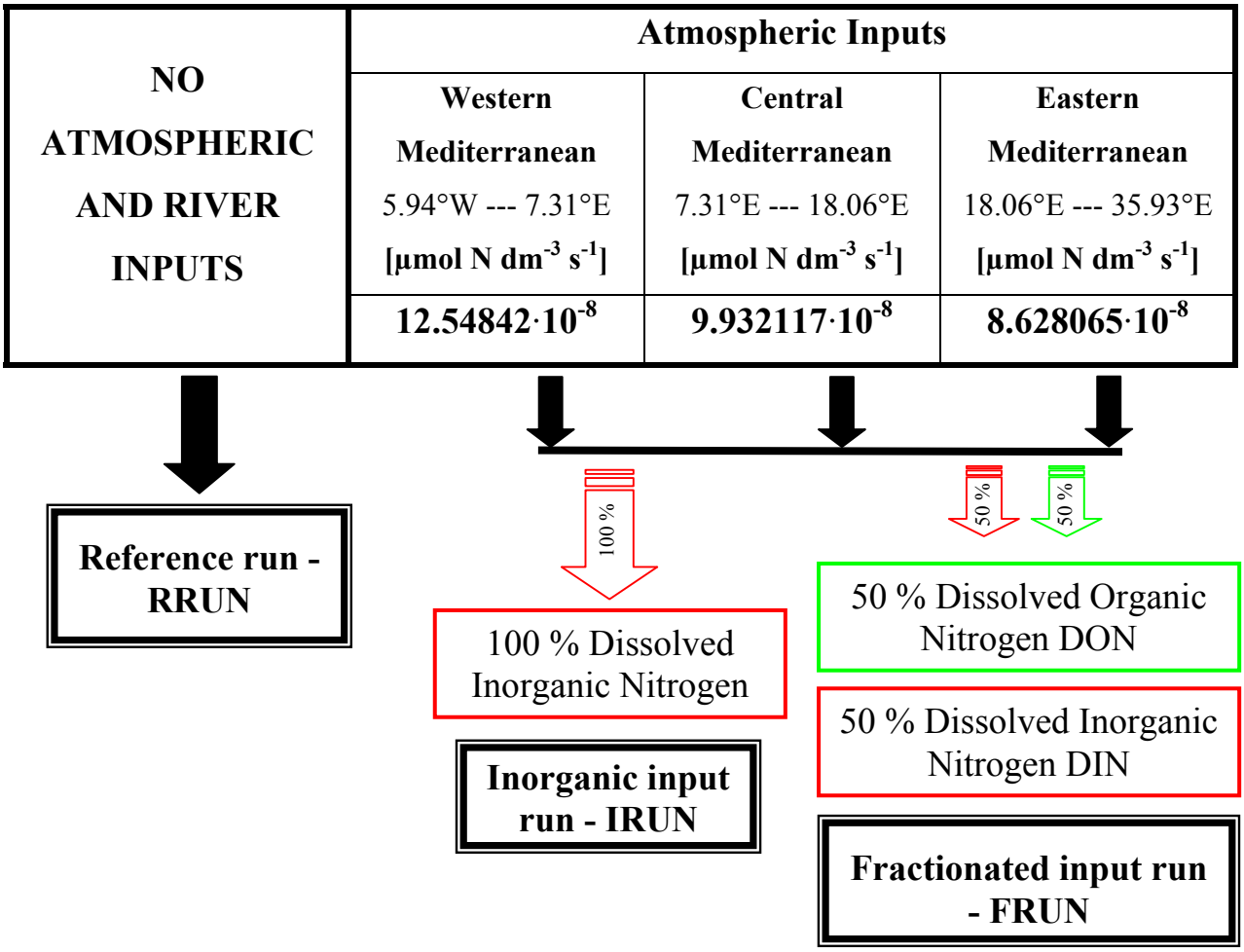

Figure 4.2. *Nitrogen loads and relative repartitions among ecological compartments. Both IRUN and FRUN are loaded with river nutrient apports.*

5. Prognostic ecomodeling

A five-variables ecomodel is the natural derivation of that one above-implemented at one eighth degree spatial resolution (Fig. 4.1), according to Mediterranean Sea experience in EC Projects like MERMAIDS, MTP II and ADIOS. This version is going to be used as data generator in multivariate twin experiments. The resolution of the trophic web for this purpose is obtained with good

parameterization of the effective processes in the lower trophic levels, and reducing the higher trophic ones to the pressure of only one generalized secondary producer, which closes the ecosystem. This choice gives raise to systems with a limited number of compartments, like those applied for depicting in JGOFS the impact of the nitrogen fixation in Atlantic or the interplay between different nutrients in Pacific.

The time rate of change for phytoplankton is

$$\left.\frac{\partial P}{\partial t}\right|_{source} = G_{MAX} E(I, I_0, t) \cdot S(T) \cdot \frac{N \cdot P}{k_N + N} - d \cdot P - \gamma \cdot \frac{P \cdot Z}{k_P + P} \qquad [5.1]$$

Light attenuation due to water is

$$I(z,t) = I_0(t) e^{-k_z z - k_s \int_{-z}^{0} P dz'} \qquad [5.2]$$

where k_z=0.00034cm^{-1} and k_s=0.0003cm^{-1}(μmol N dm^{-3})$^{-1}$ from Chai et al. (Deep-Sea Res. II, 49, 2713-2745, 2002).

The uptake of chlorophyll-a, *CHL*, is given by

$$\left.\frac{\partial CHL}{\partial t}\right|_{source} = G_{MAX} \cdot E(I, I_0, t) \cdot S(T) \cdot \frac{N \cdot P}{k_N + N} \cdot \rho_{CHL} \frac{MW_C}{R_{NC}} - d \cdot CHL - \theta \cdot \gamma \cdot \frac{P \cdot Z}{k_Z + P} \qquad [5.3]$$

or, in other terms,

$$\frac{\partial CHL}{\partial t} = \rho_{Chl} P_c CHL - dCHL - \gamma \frac{ZP}{k_P + P} \theta \qquad [5.4]$$

where P_c is the photosynthesis rate expressed in nitrogen as a function of irradiance, I, and the chlorophyll:carbon ratio θ at time t (Allen, 2002):

$$P_c = P_m \left(1 - e^{-I\theta\alpha_{CHL}/P_m}\right) \cong I\theta\alpha_{CHL} \qquad [5.5]$$

where P_m is the light saturated rate photosynthesis normalized to carbon (multiplicative function of the maximum photosynthetic rate and the temperature dependence and the nutrient limitation), α_{CHL} the initial slope of the P-I curve normalized to chlorophyll (0.0000075 g C (g Chl)$^{-1}$ (μmol phot)$^{-1}$) (m^{-2}).

If the light limitation J is

$$J = G(T,N)\,p(t)\frac{I_O e^{-k_z z}}{I_{opt}} e^{(1-I_0 e^{-k_z z}/I_{opt})} \qquad [5.6]$$

the Photosynthetic Available Radiation I → 0 is

$$J = G_{MAX}\,p(t) e \frac{I}{I_{opt}} \qquad [5.7]$$

Thus the ratio is:

$$\frac{J}{I} = \alpha_{CHL} = \frac{G_{MAX}\,p(t) e}{I_{opt}} \qquad [5.8]$$

In the case of minimum I the ratio CHL/C >> 0.01, corresponding to the eutrophic situation C/CHL << 100. In the case of high I, CHL/C << 0.01 and C/CHL >> 100, oligotrophic regime is attained.

Density ρ is given by the expression

$$\rho_{CHL} = \theta_{MAX}\frac{P_c}{\alpha_{CHL} I \theta} \qquad [5.9]$$

where θ_m is the maximum chlorophyll:carbon ratio observed in cells acclimatised to extremely low light (θ_{MAX}=0.05), while θ is the plankton chlorophyll:carbon ratio at time t

$$\theta(t) = \frac{CHL(t)}{C(t)} = R_{NC}\frac{CHL(t)}{P(t)} \qquad [5.10]$$

where R_{NC} is the constant nitrogen:carbon ratio inside cells.

Three topics remain open in this treatment of the ecosystem in terms of nitrogen.

The introduction of the clouds coverage requires careful study in terms both of interannual variability and of net apport to the ecosystem response. Their input is taken into account on average by the light irradiance expression considered in the four variables model. It is possible to use this one, but only after a new optimization procedure that will consider mean unshaded light, fotoperiod, and the actual interannual variability of the clouds coverage. This last point must be taken into account by subtracting a part up to 70% of the cloud expressed in tenth.

The topic relative to adaptation must be regarded as the turbulence influence on the growth rate processes. Different parameterization of these processes can be followed; in a preliminary stage of the future work some particular constant parameterization of the decrease of the growth rate can be introduced.

Thirdly, the extension to a sixth, diagnostic or nearly diagnostic, variable as the oxygen can be a real improvement for the modeling of the Mediterraenan Sea, consisting a valuable control of all the preceding results. It remains an open question how to initialize consistently the field and how to measure the small differences of the oxygen in terms of not so long evolution of the system.

6. Winter FTE different coverages

The winter twin experiments are run with a compounded R_{SL} chlorophyll to carbon factor, equal to 1.61. This estimate is obtained considering that the small cells, comporting double factor than netplankton larger ones, compose in a different weight the community in the western and in the eastern basin. They are smaller components, about one third of the total in the Western Mediterranean; but they dominate, about thrice than the netplankton weight, in the Eastern Mediterranean. Composing these estimates with the area of the western basin, $8.6\ 10^{11}$ m^2, and of the eastern one, 16.4

10^{11} m^2, we obtain the factor given above, which is then chosen for the following experiments.

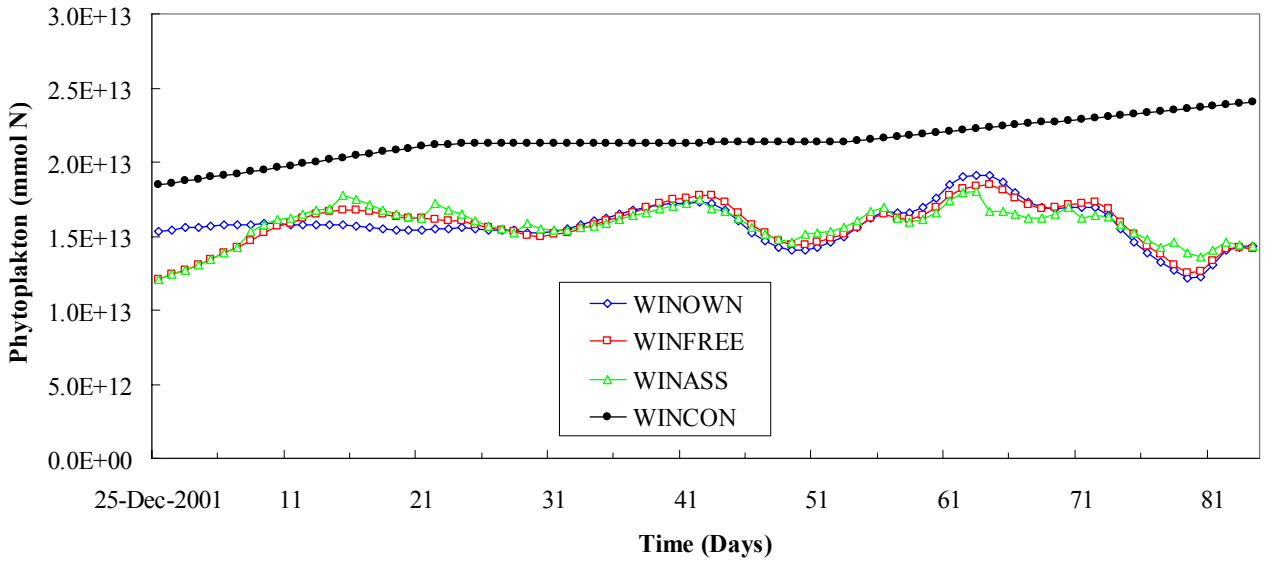

Figure 6.1. *Evolution of the phytoplankton (mmol N) in the upper 20 m layer during the winter season December 25 – March 18.*

The surface chlorophyll, inside the first two levels located at 5 m (surficial 10 m thick) and at 15 m (subsurficial 10 m thick), is the climatological seasonal cycle result in the Mediterranean sea by means of the ten variables ecosystem model (ADIOS, 2003) in the frame of MAST Projects. From one hand, this chlorophyll result is validated in terms of satellite CZCS average values at subbasin scales, those of the western and eastern basins - moreover the standard deviations remain also reasonable - from the other, this one quarter degree choice may induce further errors because of the statistical tranformation from chlorophyll to nitrogen biomass, and subsequent interpolations.

The simulated surficial, at 5 m and 15 m, chlorophyll maps are relocated at the system one eighth of degree grid; the interested surface does not cover the Atlantic box, the Adriatic buffer zone – northerly than 43°N – and the Aegean - northerly than

38°N. The interpolated weekly averages to be assimilated are given to the system at the two upper levels without transformations. After these inputs, SOFA estimates the corrections for the forecasts.

Phytoplankton corrections in nitrogen units are then obtained and applied at the GCM-NPZD level, multiplying the Kalman gains by SOFA times the reversed above-estimated phytoplankton to chlorophyll ratio.

Figure 6.1 shows the evolution of the phytoplankton content in the case of the first FTE, the one with overall coverage of chlorophyll assimilation data. Aside the unperturbed evolution, and the twin experiments, also the control run, WINCON, in terms of biomass as expressed in the following is shown. This control run remain well above in terms of surface biomass with respect both of the assimilated run, green dots – WINASS, and of the free run, red dots – WINFREE. There are differences due to the assimilation clearly seen in particular at the first stage of the evolution. These are in part hidden at the scale of Fig. 6.1 and they are well depicted in the following figures about the relative errors. Along all the twelve cycles of the simulation, there is a strong resilience not only of the WINFREE, but also of the WINASS toward the unperturbed run without any changing of the initial conditions, blue dots – WINOWN.

As introduced before, the “sea-truth” control is a monthly averaged situation. The inorganic nitrogen control concentration is given by the sum of ammonia and nitrate from this fraternal climatological run; the phytoplankton one is the sum of the ultraplankton and of the netplankton; the zooplankton and the detritus are the corresponding concentrations in the fraternal ecomodel; chlorophyll surface variable is diagnostic and validated at basin scale versus CZCS monthly average maps. Because the fraternal ecomodel is at one quarter degree, the control data are interpolated for giving their one eighth degree counterparts in terms of assimilated chlorophyll data and “sea-truth” situation. The procedure is linear in time for giving daily concentrations necessary for the following relative error statistics.

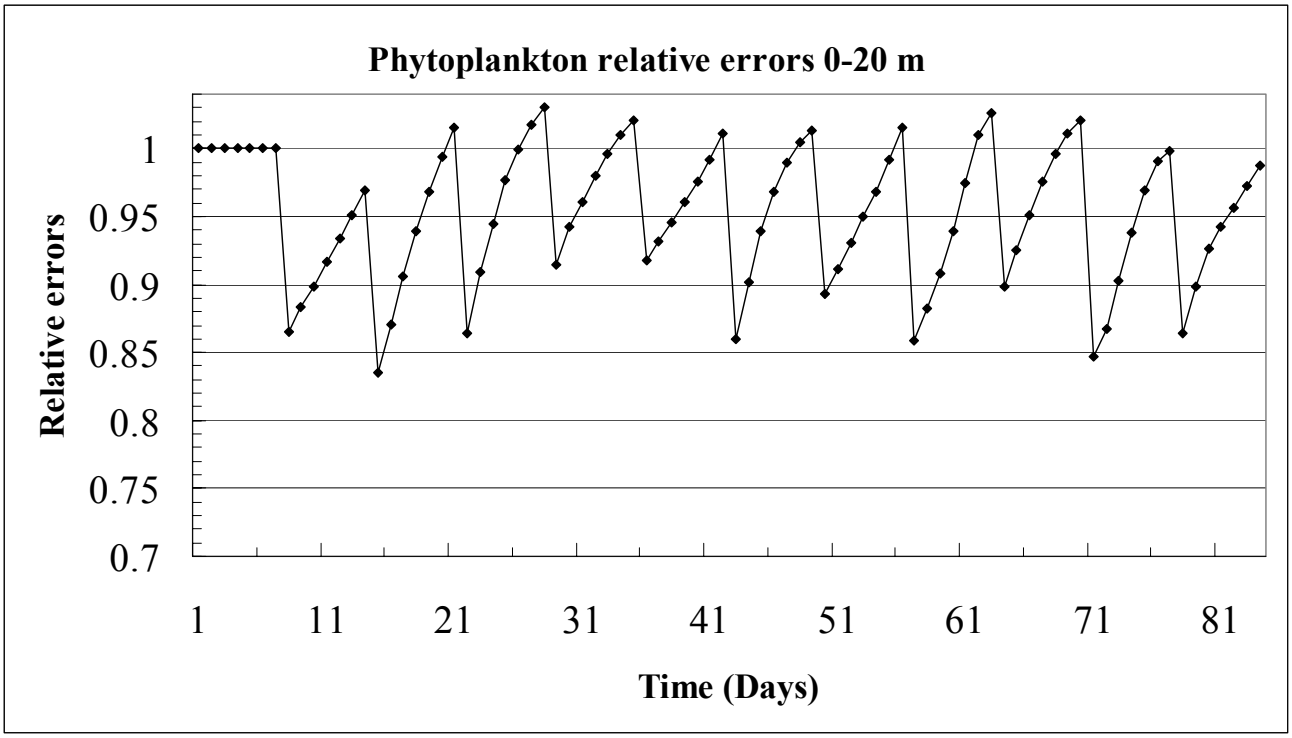

Figure 6.2. *Phytoplankton relative errors evolution in the 0-20 m surface layer during the 84 days of the evolution.*

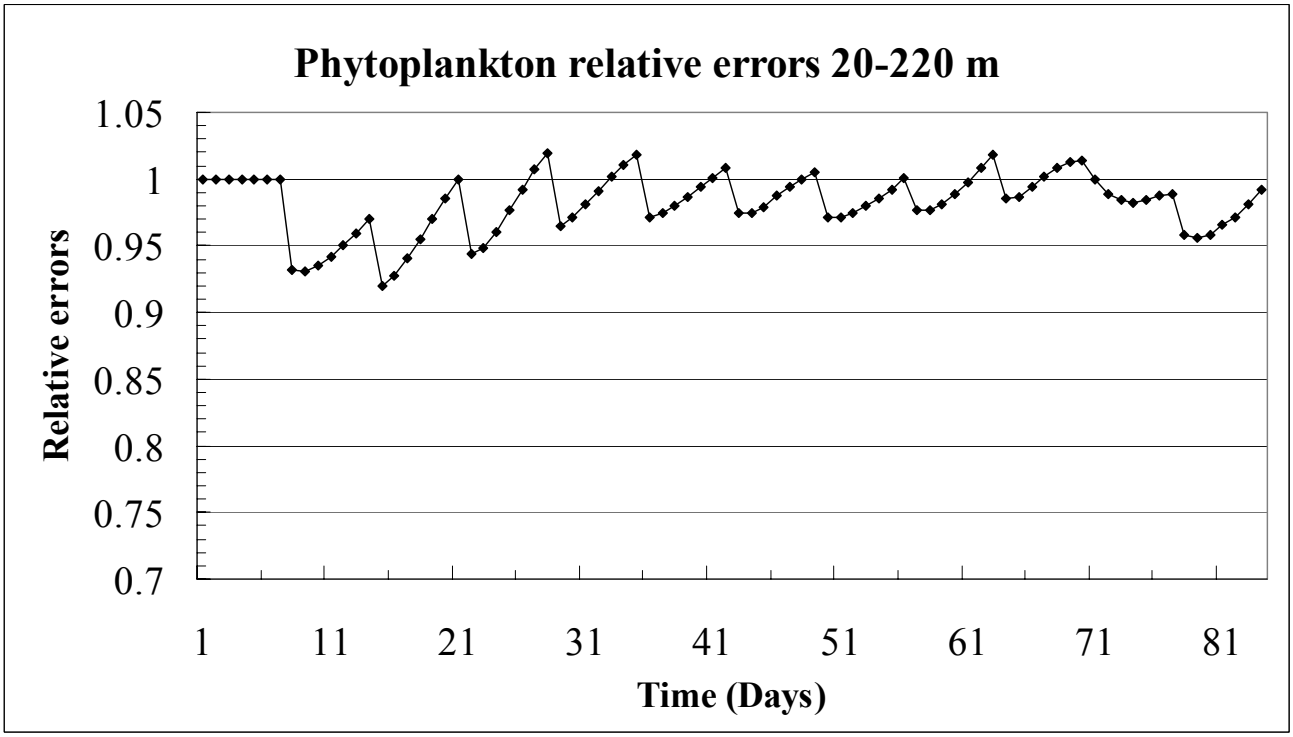

Figure 6.3. *Evolution of the phytoplankton relative errors in 20-220 m layer.*

The phytoplankton relative errors generally decrease after the total coverage assimilation cycles during this winter season evolution. In Fig, 6.2 the relative errors at the 0-20 m level are shown along the 84 days, after twelve assimilation cycles. The value decreases to 0.85 after each assimilation step. After five days it returns to values about one, with no improvements with respect to the free run. This is also clear by the close evolution of the superficial phytoplankton content, not shown, where the control run remains well above the assimilated, and the free one.
The interior phytoplankton relative errors, Fig. 6.3, are representative of the subsurficial evolution from 20 m to 220 m depth. The improvement of the error due to the assimilation – total coverage – made only at surface, thus completely outside this level, is no more than 5%. There is increase after four-five days toward free run evolution and some other similarities with Fig. 6.2: at the beginning a slight better forecasting is obtained, as seen at surface, and the same at the last cycles of the simulation. An intermediate behaviour is given by the phytoplankton relative errors in the water column, Fig. 6.4. The oscillations are here more or less by 5% in amplitude, with some significant loss of forecasting near the end of each cycle.

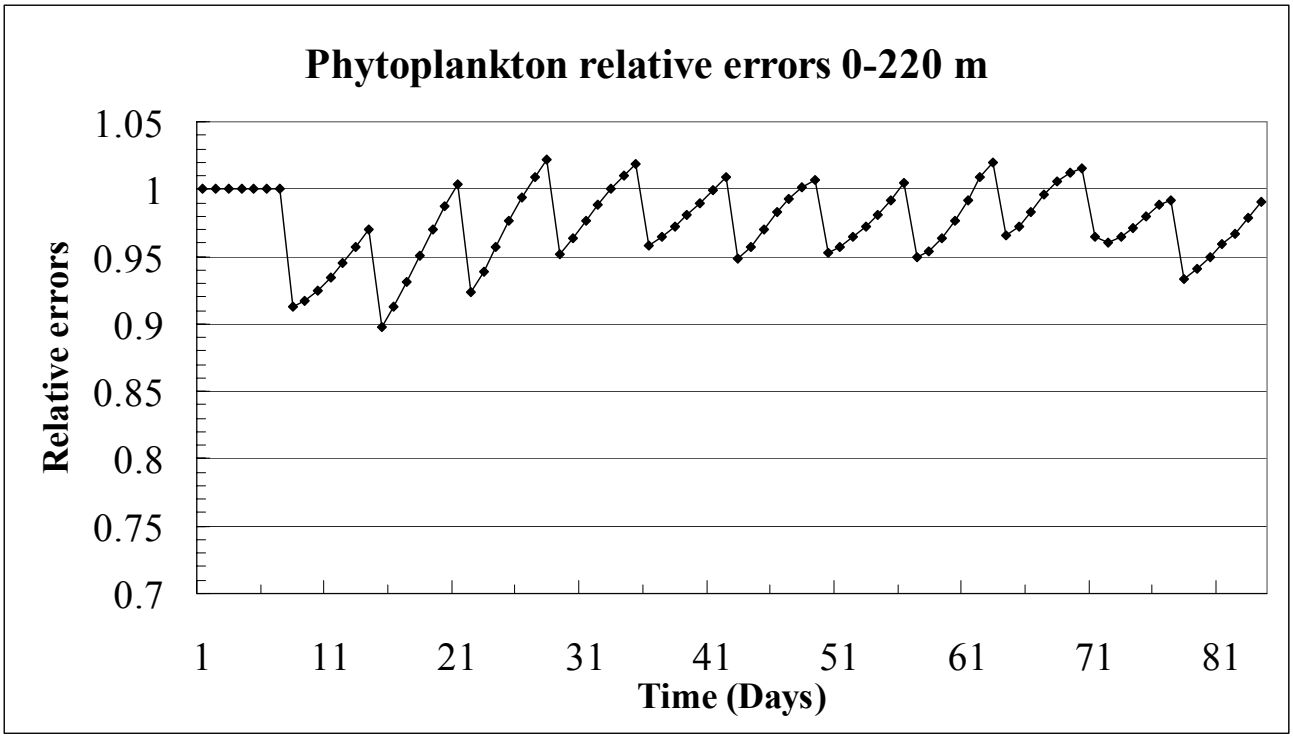

Figure 6.4. *Evolution of the phytoplankton relative errors in the 0-220 m layer.*

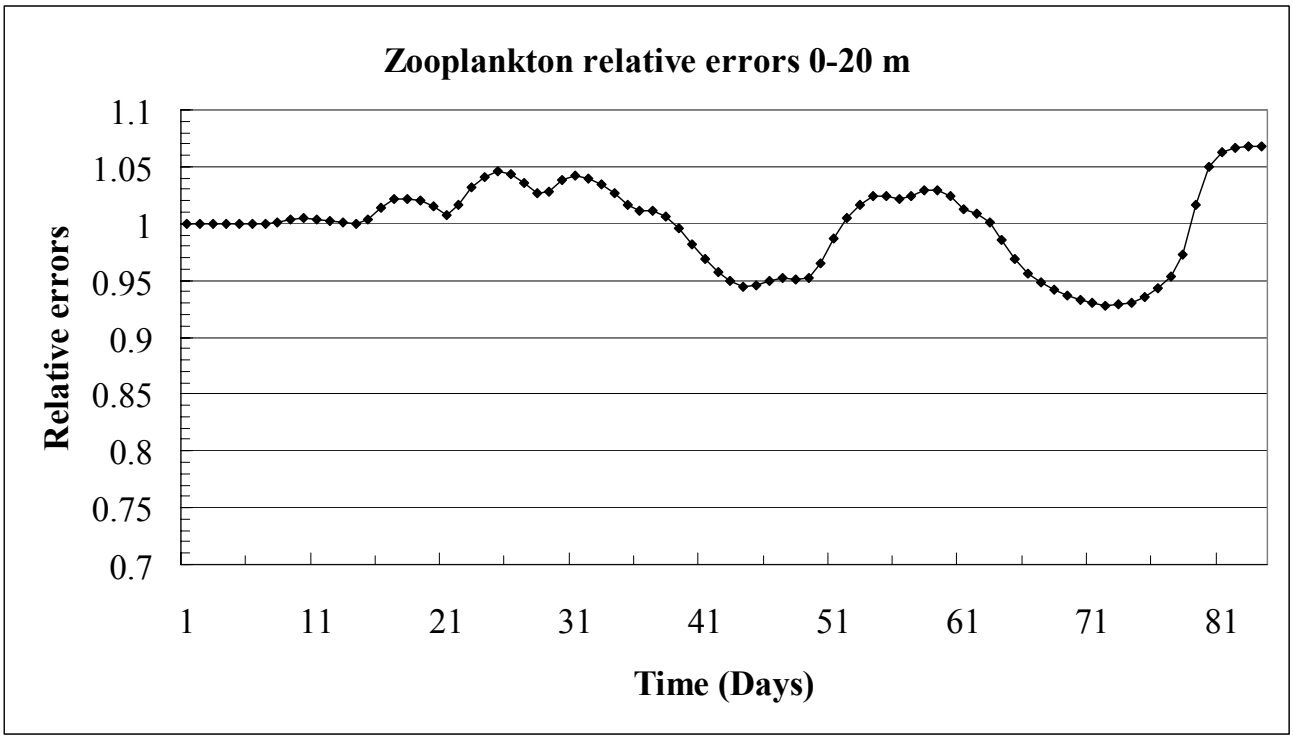

Figure 6.5. *Evolution of the 0-20 m zooplankton relative errors.*

The evolution of the zooplankton relative errors is shown in Fig. 6.5. After some decrease of the forecasting performance, i. e. relative errors higher than one, better scores are evident in the central part of the FTE. In any case, it is impossible for this FTE to recover better zooplankton performances at the end of the run. Interestingly we note some positive reaction to the assimilation in the inorganic nitrogen relative errors, Fig. 6.6, and even more pronounced in the detritus relative errors, Fig. 6.7.

0-20 m inorganic nitrogen evolution begins with a nearly neutral error, which turns to better forecasting of this variable after about twenty days. It is worth noting that it remains slightly better after assimilation till the last week of the run, always with 3-4% increase. Upper layer detritus is even more pronounced: the improvements

in detritus forecasting is a net 4-5%, but here they remains nearly constant for all the FTE.

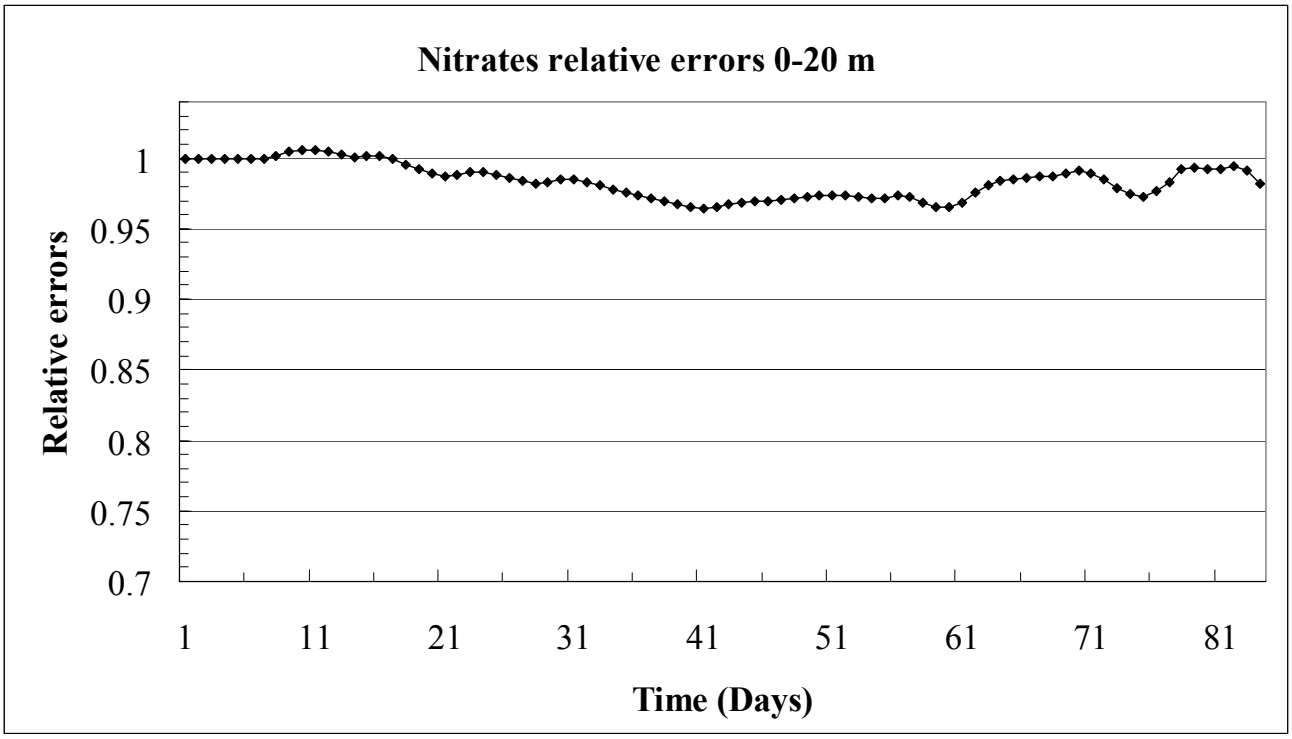

Figure 6.6. *Evolution of the 0-20 m inorganic nitrogen relative errors.*

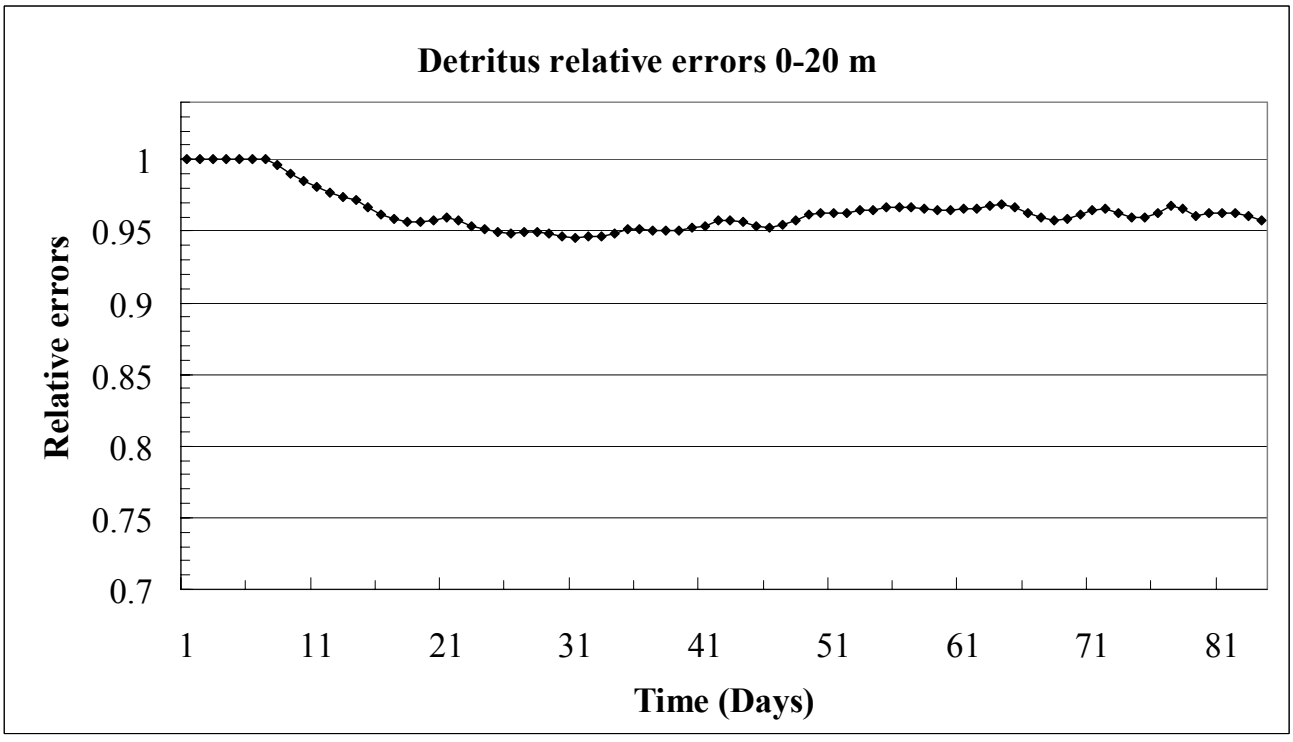

Figure 6.7*. Evolution of the 0-20 m detritus relative errors.*

The total nitrogen relative errors are shown in Fig. 6.8 for the upper layer 0-20 m. Here the forecasting improvement is more than 5% and during the simulation it increases. It is worth noting the different behaviour of this FTE in comparison with the ITE reported in the first MFSTEP technical report (MFSTEP WP6-D5, 2004). The winter period is characteristic of both experiments and the analyses must give a thorough understanding of dissimilarities. It is possible that in the FTE the western basin is dynamically adjusting to higher, more realistic, values of the total nitrogen and this process is recognized as better performances against the "sea-truth" control which is more similar to the climatological nutrient availability in the upper layer.

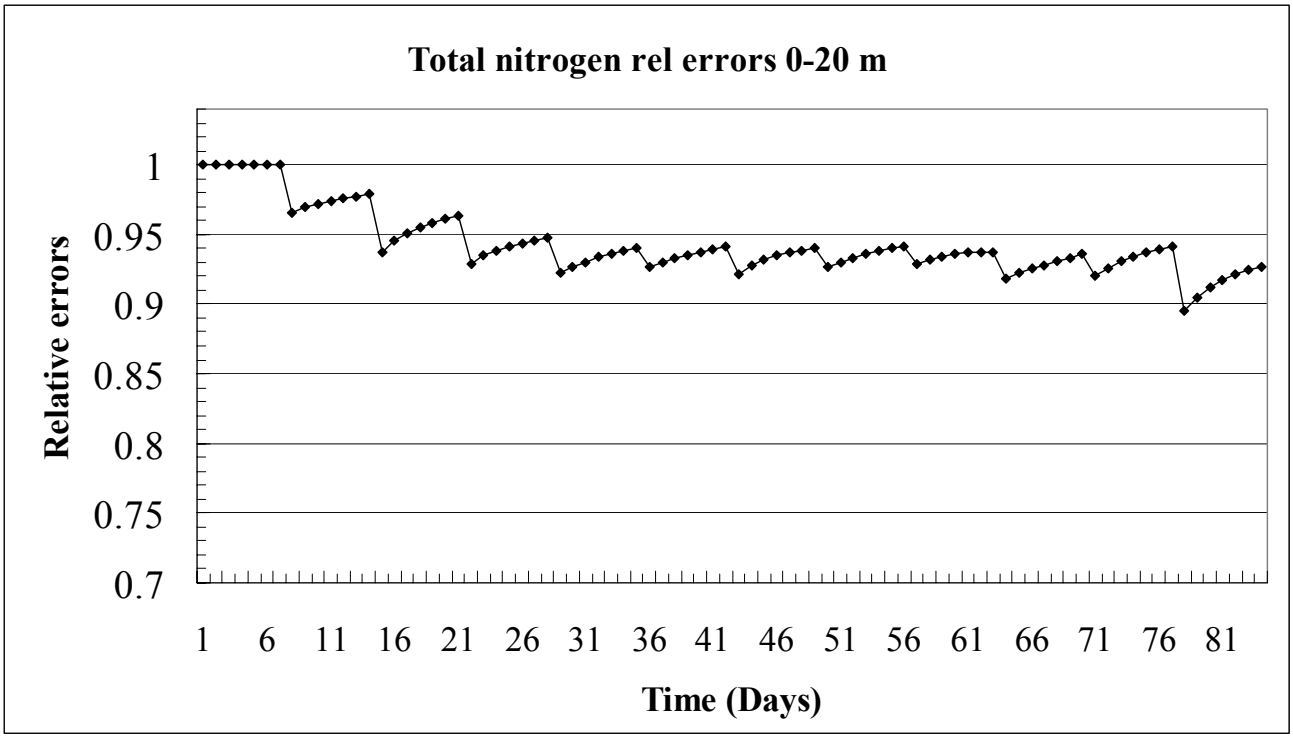

Figure 6.8. *Evolution of the 0-20 m total nitrogen relative errors.*

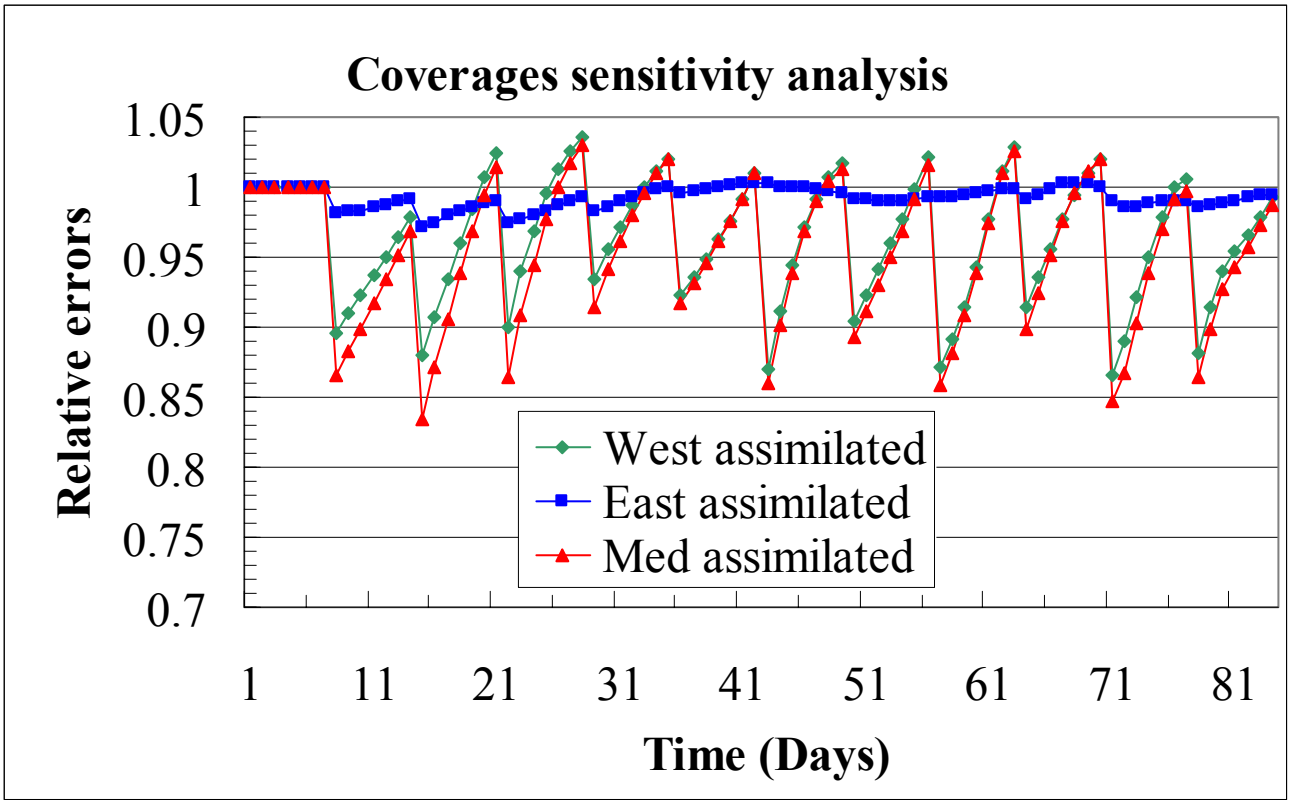

Figure 6.9. *FTE winter sensitivity in the 0-20 m level to three different chlorophyll fields assimilated in the SOFA scheme. Red triangles are the phytoplankton relative errors in the case of total Mediterranean chlorophyll coverage; green diamonds and blu squares are respectively the relative errors after only western and only eastern chlorophyll assimilation.*

It is interesting to point out the importance of different chlorophyll coverages in separated assimilation experiments [Fig. 6.9]. As said before, we chose three different assimilated inputs: the total Mediterranean chlorophyll coverage that gives rise to the results shown before from Figg. 6.2 to 6.8, and the two other "sea-truth" coverages, where alternatively eastern basin surface chlorophyll and western basin are blank. These two situations correspond, in certain sense, to possible winter cloud coverage of all the Eastern, or respectively Western Mediterranean, during all the weekly period in which forecasting external data are taken. In the case of western data only, the results do not differ from the total Mediterranean coverage. Only

minima sometimes differ, while maxima and evolution shape are very similar also in values. This suggests the important role assumed by the western basin on average and for the errors. The blue squares in Fig. 6.9 represent the relative errors evolution in the case of only Eastern Mediterranean chlorophyll assimilation. The corrections do not exceed 2-3% as maximum gain. These maxima are reached in correspondence with the differences about the total and western coverages. We interpret this sensitivity result as a complementarity of the two basins. Moreover the correction imported by the western basin can be in the majority of the cases higher than the eastern one: firstly the western basin admits a yearly average range with values about double than in the Eastern Mediterranean; moreover corrections of the data can be well introduced in the features seen by satellite while in the eastern part these cannot be evidenced by remote processing because signature of prevalenty low anticyclonic patterns.

7. Summer FTE responses in the basins

Some testing of analogous techniques in summer stratified conditions are reported in the present and in the following section. Firstly we perform twin experiments with the summer initial conditions, for the phytoplankton only, modified to winter initial conditions shown in the preceding section. Secondly, in the eighth section, we communicate the response of the optimal interpolation inside the own evolution of the system, i. e. simulation of the “assimilation” of the “satellite data” in the integrated system.

The summer FTE, reported in this paragraph, with winter interchanged conditions at place of the summer natural ones, has been performed to understand how the biological assimilation scheme is affected by the stratified vertical structure of the water column. Thus we perform the experiment with the summer

phytoplankton initial conditions modified into winter initial conditions taken from the 25th of December biomass field shown in the preceding FTE. Also the period of this experiments is 84 days, twelve assimilation cycles, starting on the 25th of June and ending at September 16. The assimilated surface chlorophyll, also here at 5 m and 15 m depths, is relative to the summer period of the control run and is assimilated at the end of each week.

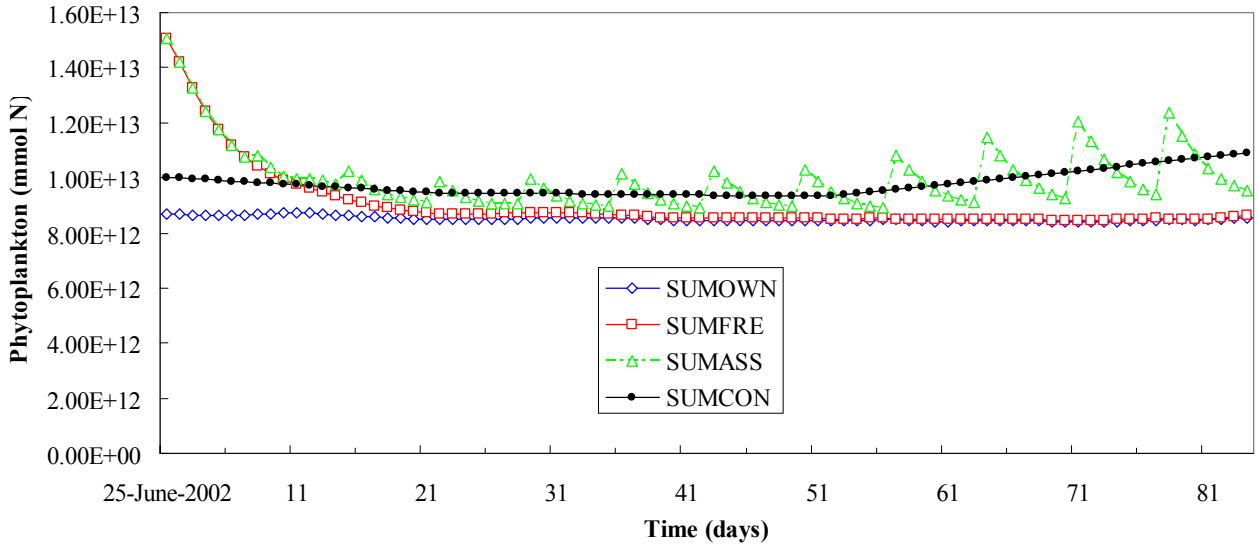

Figure 7.1. *Evolution of the phytoplankton content (mmol N) in the upper 20 m layer during the summer season June 25 – September 16. SUMOWN, blue diamonds, represents the evolution of the imperturbed run. SUMFRE, SUMASS, and SUMCON represent respectively the evolutions in the case of the free run, modified winter initial conditions, of the assimilation run, modified I. C. plus assimilation of the summer surface chlorophyll, and the phytoplankton control biomass transformed from carbon to nitrogen units.*

In Fig. 7.1 the total phytoplankton is shown for the own pre-conditioned NPZD simulation for the summer period from June 25 to September 16 in the upper 20 m.

This blue evolution, SUMOWN, shows during the 84 days a nearly flat phytoplankton, estimated in nitrogen content. The red evolution, free experiment - SUMFRE, and the green one - SUMASS, assimilated experiment starting from winter conditions typical of the December 25 run, start from 60% biomass more than the own-conditioned one in the 0-20 m level.

After about two weeks, the SUMFRE converges toward the SUMOWN. The SUMASS remains well above the SUMFRE, with higher peaks in the weekly performed assimilations and lower distance away from them. In every case, the SUMASS remains well around the average values of the sea-truth SUMCON, in Fig. 7.1 black points.

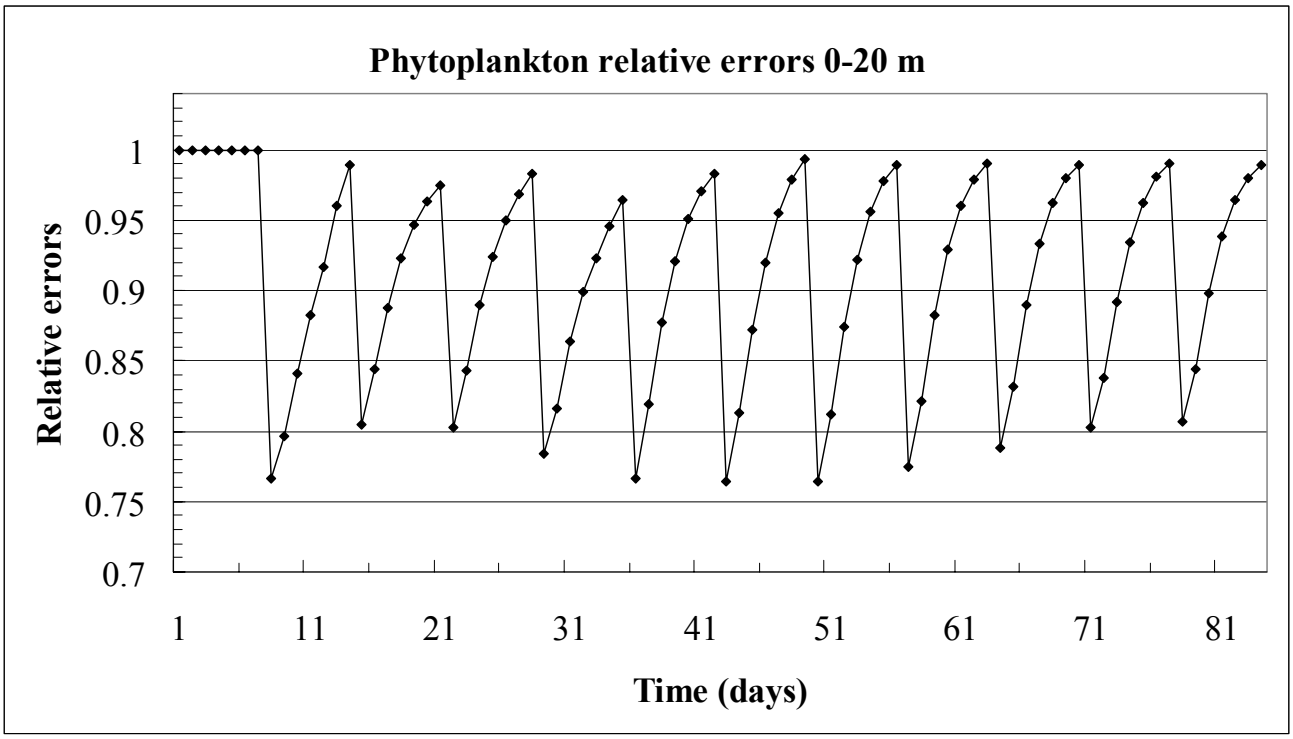

Figure 7.2. *Phytoplankton relative errors evolution in the 0-20 m surface layer during the 84 days of the evolution.*

The better forecasting increase, due to the assimilation of the control chlorophyll data at surface, is described daily by the phytoplankton relative error in

the same 0-20 m level, Fig. 7.2. At each assimilation cycle the error of the assimilated run decreases with respect to the free one. The performance is better every week of a 20% amount. Afterwards there is, in the non-assimilating day of the week, an increase of this relative error, showing the resilience of the subsystem in about five days, before the following cycle of the assimilation. The relative errors remain below the unitary sill for all the simulation, indicating that there is always in this experiment an improvement in the SOFA efficiency.

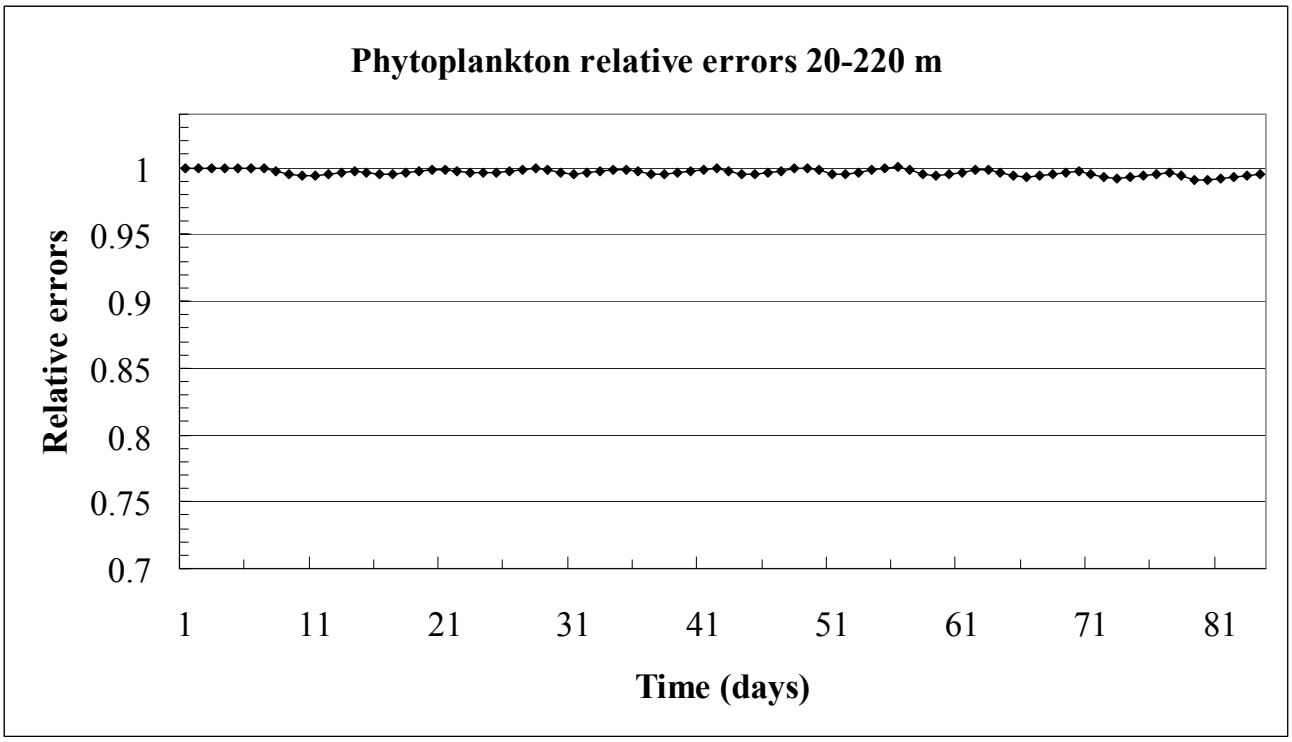

Figure 7.3. *Evolution of the phytoplankton relative errors in 20-220 m layer.*

Also in the part of the basin not assimilated in terms of chlorophyll data, a better, but very small, improvement of the errors is attained immediately after the assimilations [Fig. 7.3]. The influence of this correction is in this case of less than 2% of the free values, indicating that the water column processes transport very slowly the new informations introduced at surface.

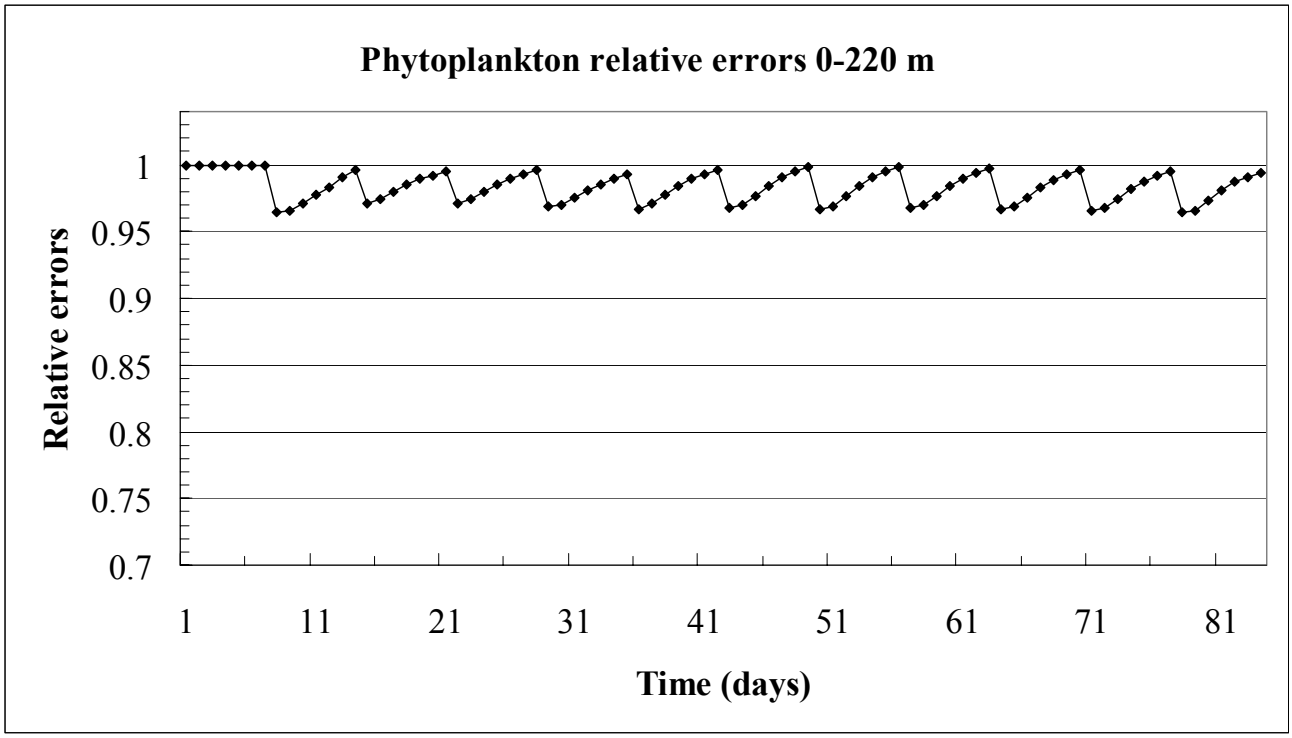

Figure 7.4. *Evolution of the phytoplankton relative errors in the 0-220 m layer.*

The summary of the two above-introduced figures is given in Fig. 7.4. This gives the reaction of the phytoplankton relative error in the water column to the upper layer assimilation. The overall assimilated biomass is better than the free one of about 5%. The weekly cycle reach nearly one after 5 days, as in the 0-20 m evolution [Fig. 7.2].

The zooplankton relative errors are drawn in Fig. 7.5. After some preliminary oscillation in the first 20 days of the simulation there is a continuous increasing of the errors in the central and last part of the SUMASS with respect to the SUMFRE. The errors are 30% worse about near the end of the 84 days. Zooplankton variable takes all the loads of the biomass increase due to the chlorophyll assimilation toward control data of Fig. 7.1.

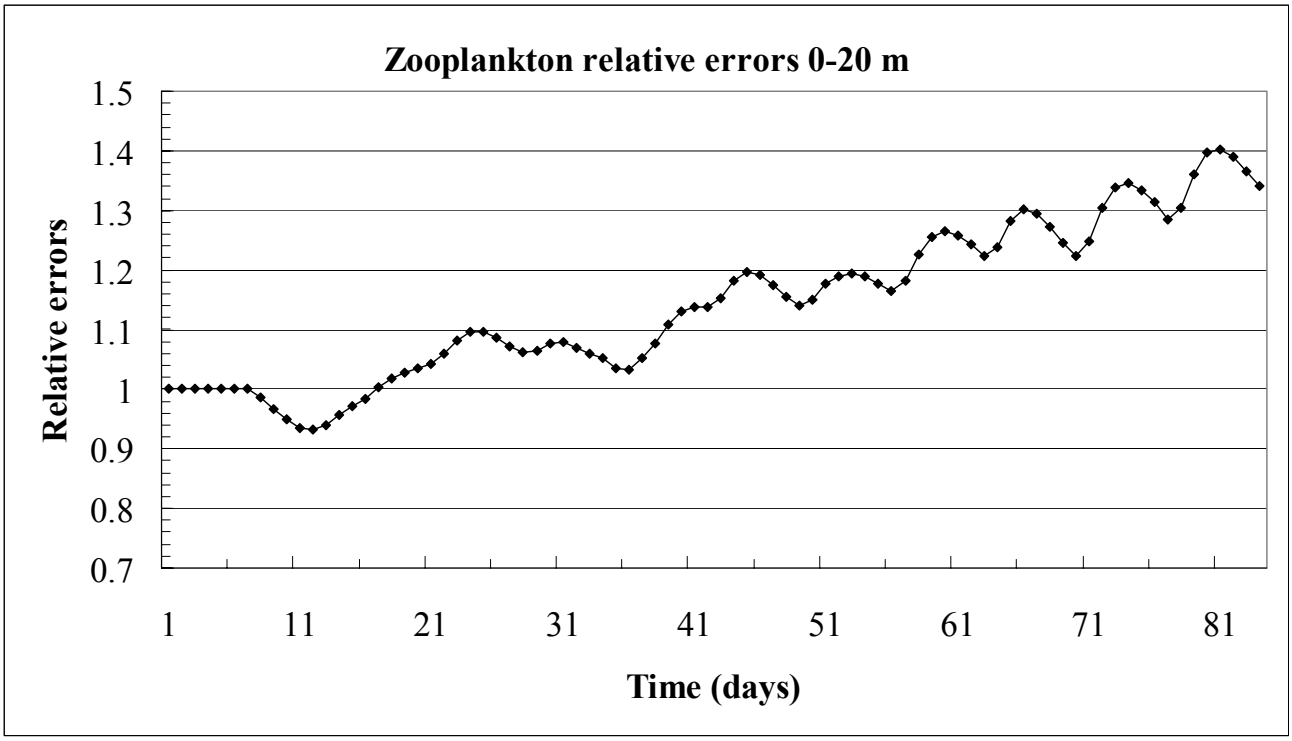

Figure 7.5. *Evolution of the 0-20 m zooplankton relative errors.*

On the other hand, 0-20 m inorganic nitrogen relative errors shown in Fig. 7.6 and, even more clearly, detritus relative errors in Fig. 7.7 are nearly neutral. Thus these two variables do not attain some sort of better forecasting in any time of the simulation, indicating that the overall simulation perform some better estimation of the phytoplankton, a worse one of the zooplankton. Total nitrogen relative errors (Fig. 7.8) run well in terms of the 84 days of the simulation; the interpretation of this fact relies, as previously indicated, in the long-time stabilization of the total nitrogen content, in particular in all layers – superficial, intermediate, deep – of the Western Mediterranean Sea (Crispi and Pacciaroni, 2005).

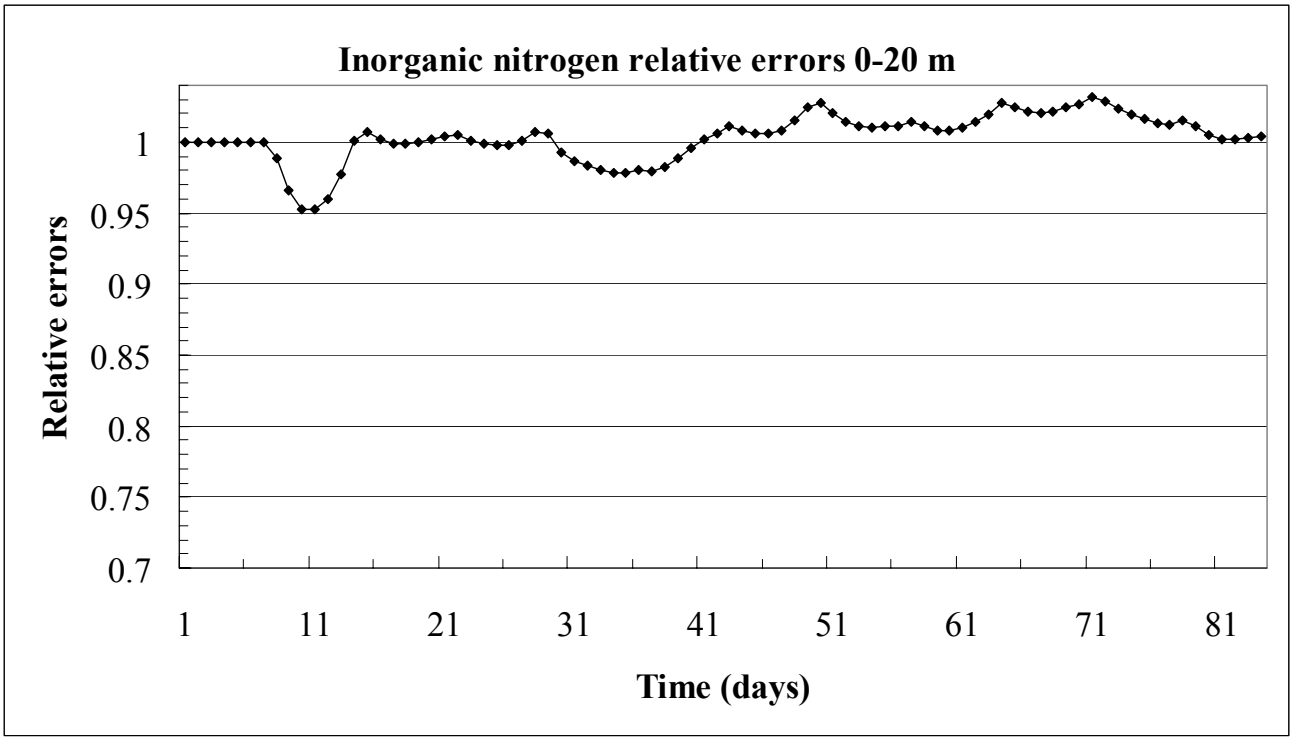

Figure 7.6. *Evolution of the 0-20 m inorganic nitrogen relative errors.*

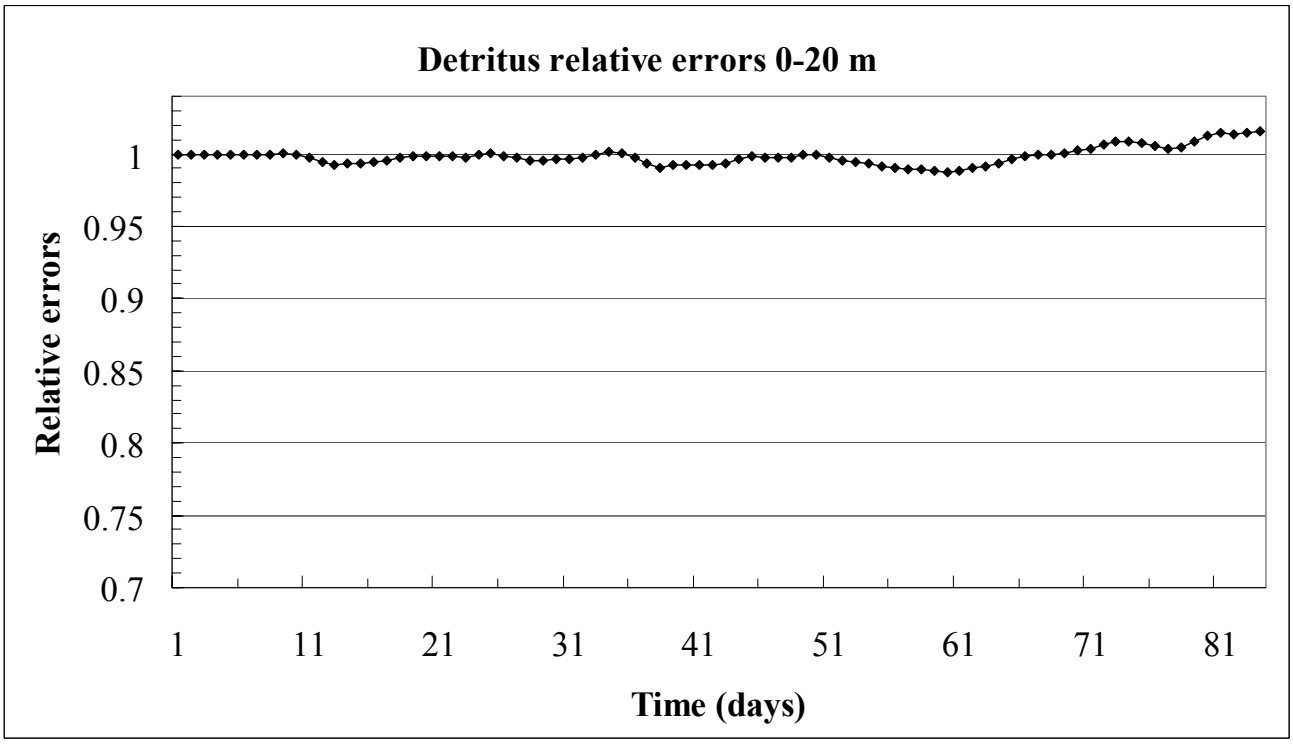

Figure 7.7. *Evolution of the 0-20 m detritus relative errors.*

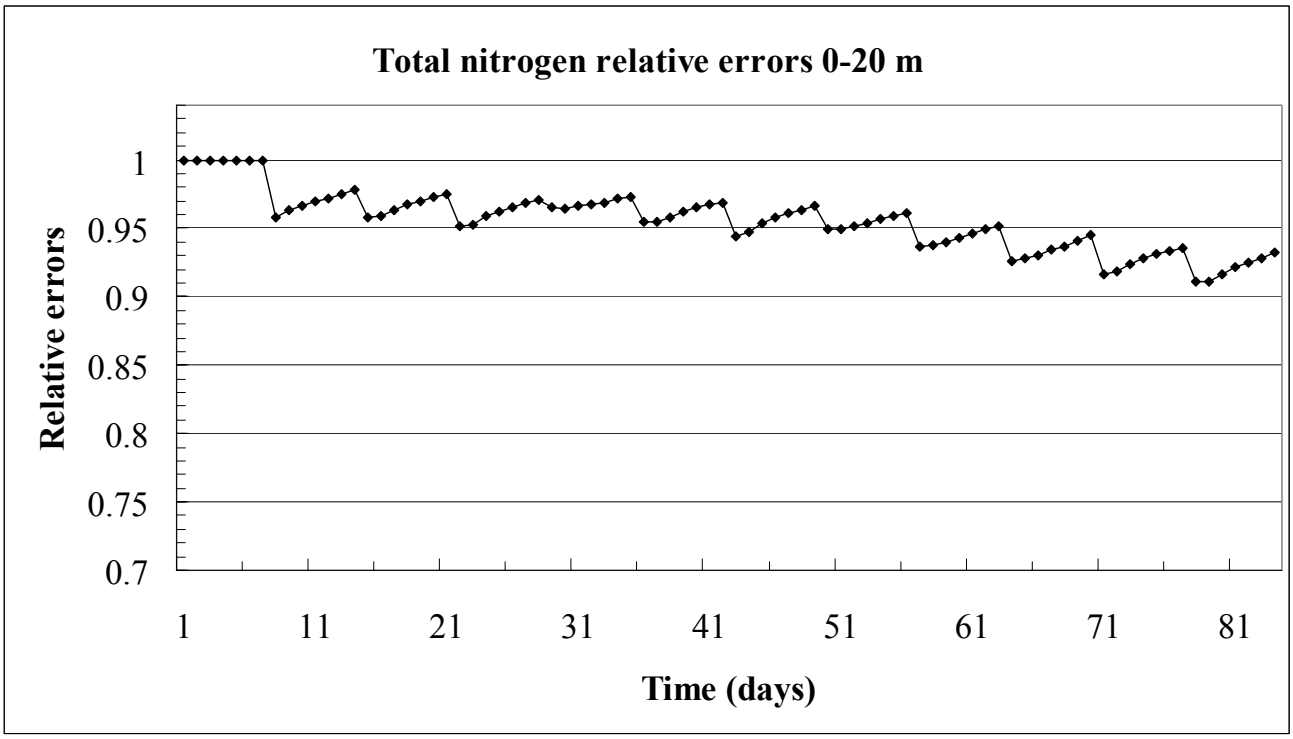

Figure 7.8. *Evolution of the 0-20 m total nitrogen relative errors.*

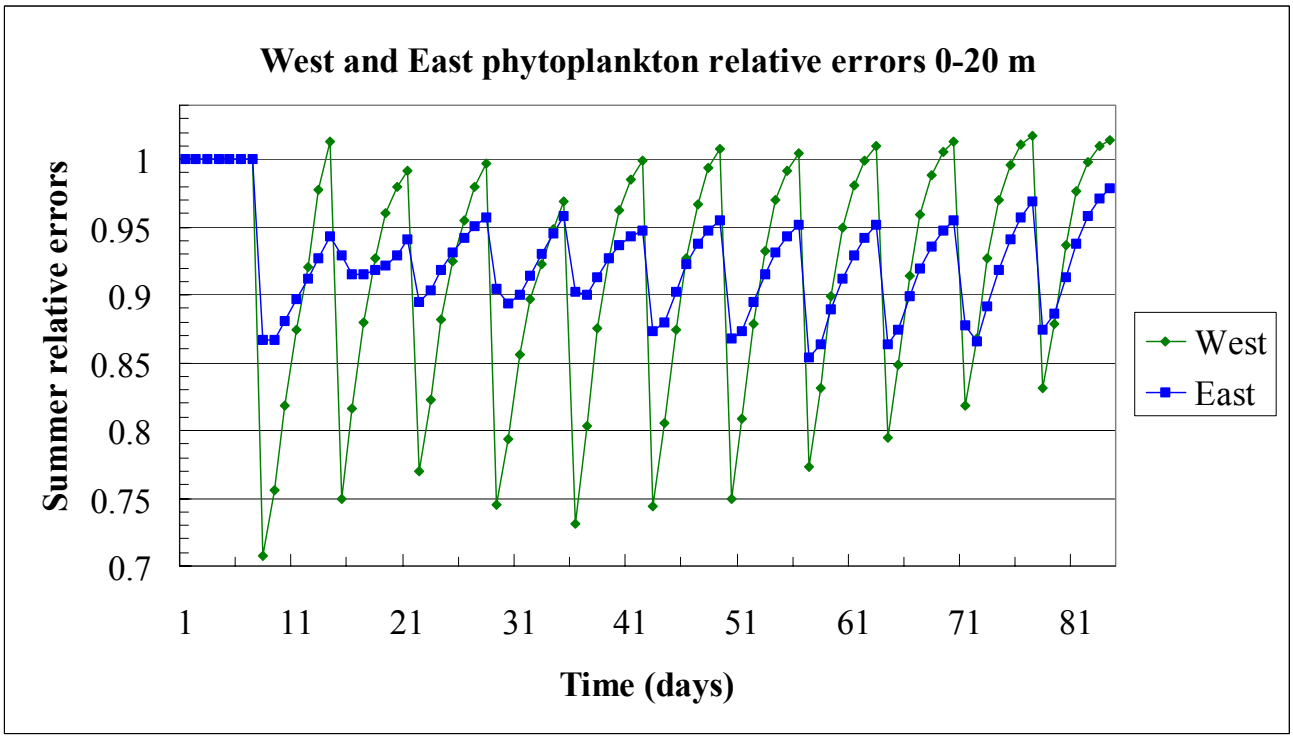

Figure 7.9. *Summer evolution of the 0-20 m phytoplankton relative errors in the western (green) and in the eastern basin (blu).*

Figure 7.9 shows the phytoplankton relative errors in the upper layer, from surface to 20 m. The calculations are here performed on the two different subbasin domains: blue squares for the western basin, green diamonds for the eastern one. It is evident the stronger resilience of the western basin, in which the informations introduced by the biomass assimilation are cancelled in four or five days; otherwise they are maintained, with the forecasting improvement of more than 5% on average, in the eastern basin. This can be originated by the mixed layer turbulent processes, certainly more intense in the Western Mediterranean than in the Eastern Mediterranean, subject mainly to anticyclonic regime.

The analogous winter result is given in Fig 7.10. The 84 days of the free, summer reinitialised phytoplankton, run is compared with the assimilated one, overall basin assimilation. The western evolution, green dots – West, are well in line with the Fig. 7.9 result obtained with the winter dynamics; while the eastern evolution, blue dots – East, exhibits a very different behaviour. Also in this latter case the resilience is obtained during the winter season indicating that it is exactly the mixing processes, highly acting during the winter not only in the Western Mediterranean but also in the eastern basin, to trigger this memory mechanism.

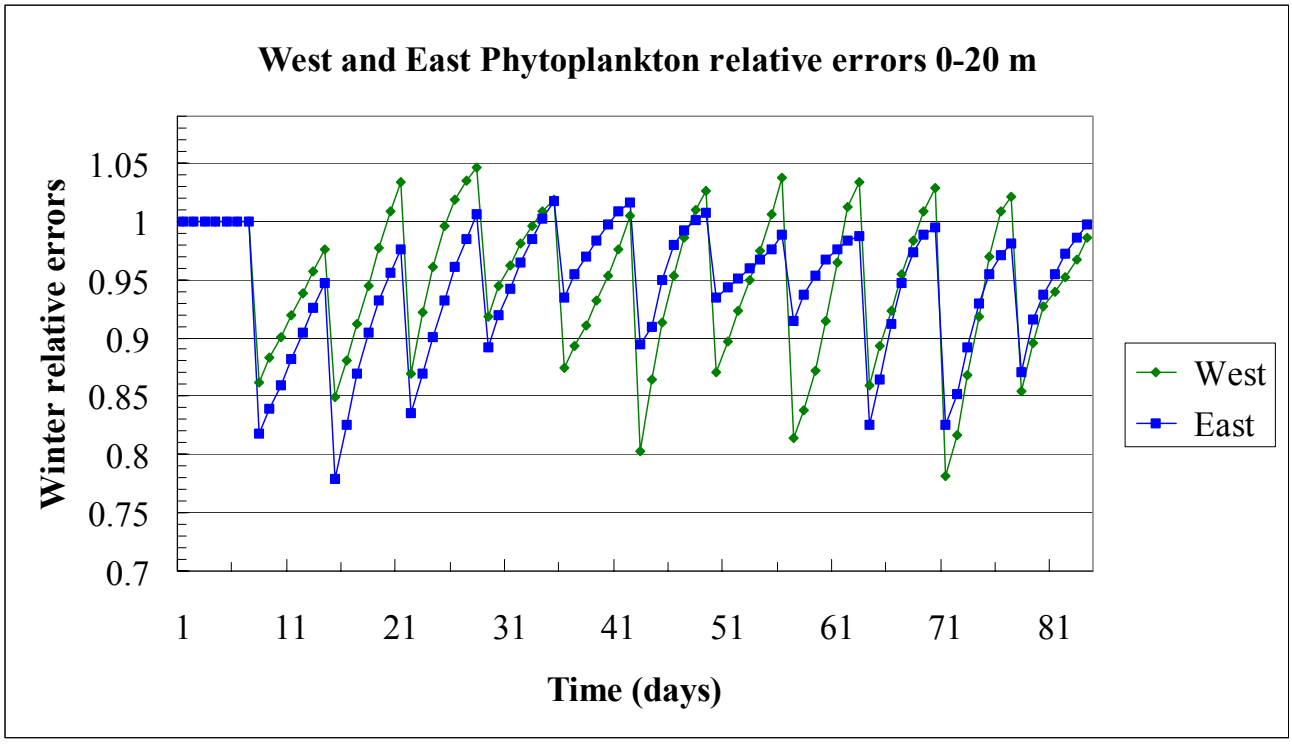

Figure 7.10. *Winter evolution of the 0-20 m phytoplankton relative errors in the western (green) and in the eastern basin (blu).*

8. Example of summer assimilation

In the following experiments we will continue the summer season. This period span from the 25th of June to the 16th of September and the forcing period is always taken from the hourly 1998 ECMWF database.

In this last numerical experiment we treat the results of the assimilated process inside the reference run evolution without any modification to the initial conditions.

The chlorophyll data are taken from the ECHYM outputs (ADIOS, 2003), interpolated at one eight of degree, and averaged at the end of the week - at the 2nd of July, at the 9th of July, etc. – and assimilated at the end of all the 12 weeks after a transformation from chlorophyll to nitrogen biomass.

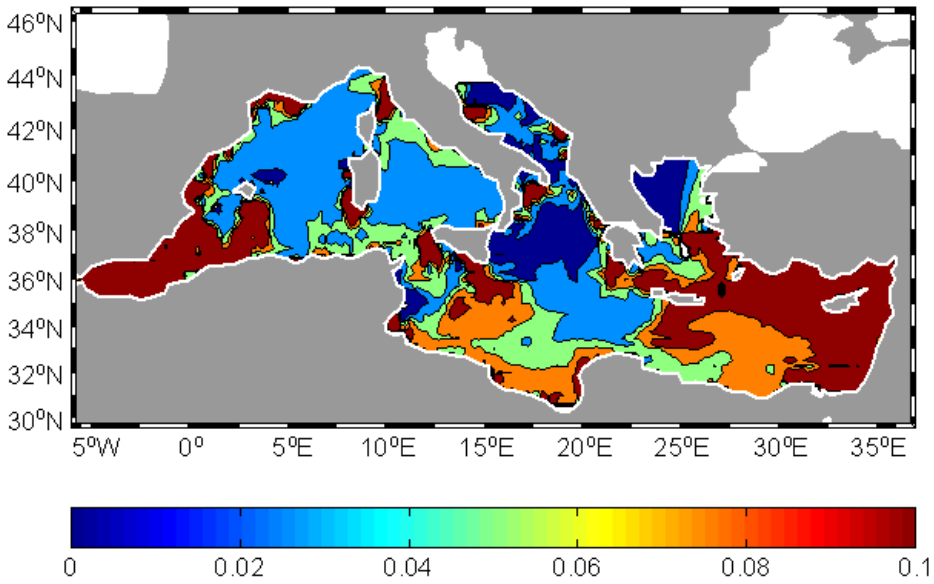

Figure 8.1. *Distribution of the chlorophyll content (mg Chl m^{-3}) from the control run. Northern Adriatic above 43°N is blank.*

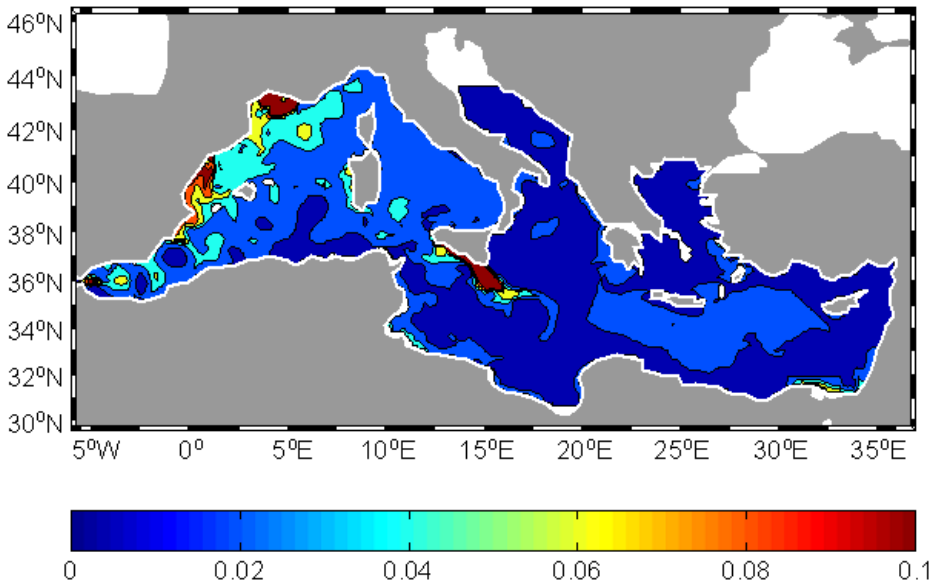

Figure 8.2. *Reference run chlorophyll distribution (mg Chl m^{-3}). Northern Adriatic above 43°N is blank.*

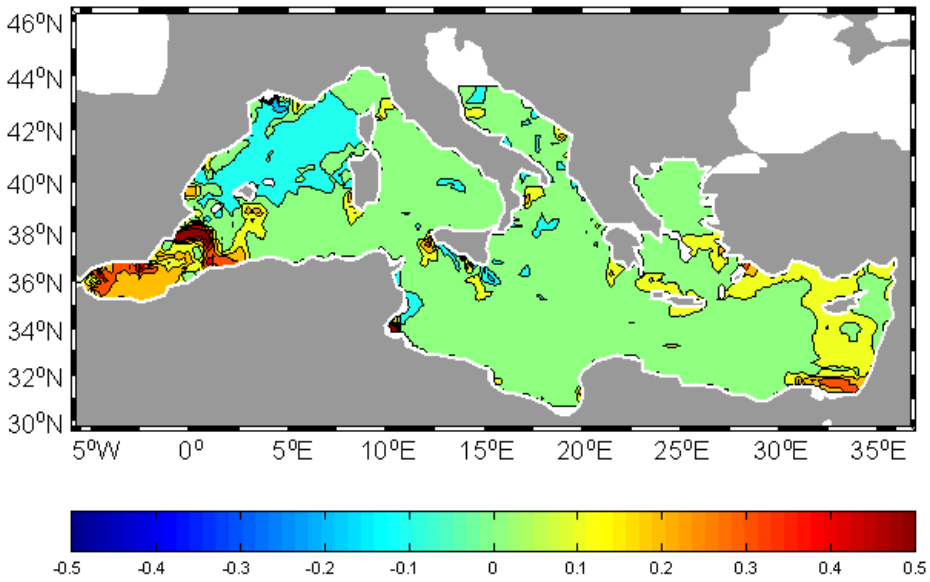

Figure 8.3. *Chlorophyll differences between control and reference run. Northern Adriatic above 43°N is blank.*

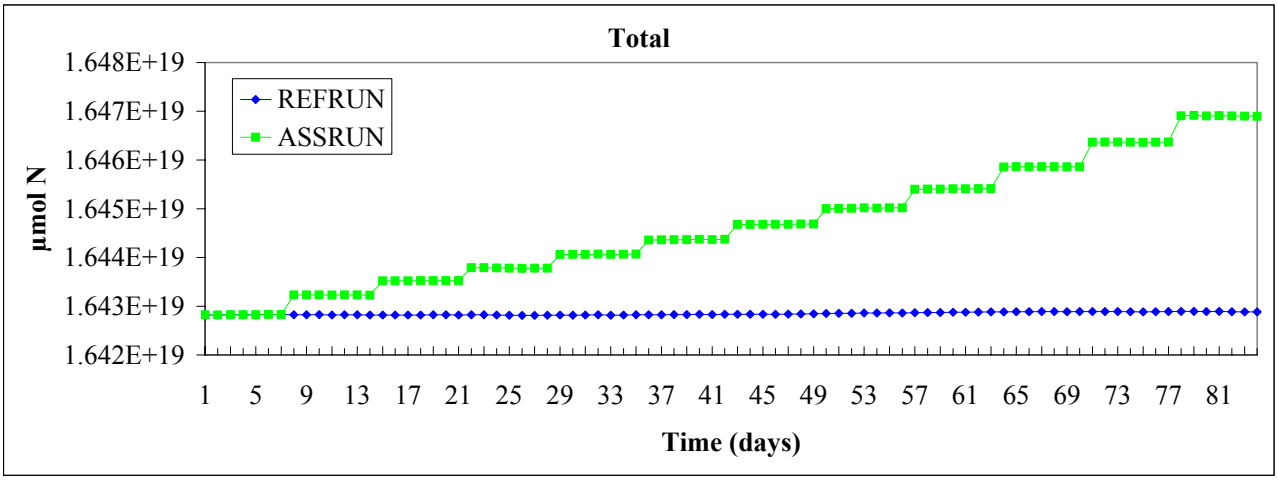

Figure 8.4. *Total nitrogen content from surface to bottom in the Mediterranean Sea, considering reference (blu dots) and assimilated run (green dots).*

In Figure 8.4 the evolution in the Mediterranean of total nitrogen, sum of nitrate, phytoplankton, zooplankton and detritus, along the 84 days of the experiment is shown. It is recognizable in Fig. 8.4 a clear stability of the reference run.

Atmospheric and rivers boundary conditions balance the nutrient net outflow of nitrogen at Gibraltar Strait. This is confirmed also by the euphotic content in the upper layer, which maintain approximately its value and therefore the conditioning factors of the biochemical cycle. This evolution contrasts with the continuous increasing of the assimilated run due to the introduction of new biomass at surface not-compensated by rich–nutrient outflow. There is a strong impulse at each assimilation cycle, with some increase of these steps at the end of the run; after every assimilation kick the response is nearly constant.

The motivation of this trend is explained by the phytoplankton response given in Fig. 8.5a. In these summer conditions the overall phytoplankton is nearly flat conserving its biomass in nitrogen units. Anyway it is evident that corrections are always positive, indicating that the innovation between data and model is always positive, as seen before for the first assimilation cycle. Anyway there is a resilience of the assimilated run toward the reference before a new assimilation period; it is hard to see any clear convergence of the assimilated run. For what concerns the zooplankton, see fig. 8.5b, there is a strong increment with respect to the reference evolution, where the zooplankton is losing about 25% of its biomass in the considered summer period. This effect is entirely due to the strong increasing of the phytoplankton average and thus of the grazing upon the higher biomass.

Nitrates remain nearly constant for the first four cycles, see Fig. 8.6a, because the moderately higher uptake is equivalent to the zooplankton excretion. In the last cycles nitrate grows for the detritus higher remineralization. This last compartment exhibits a continuos relative increase in the assimilated run with respect to the reference one for the effect of the mortality of the overall biomass, see fig. 8.6b.

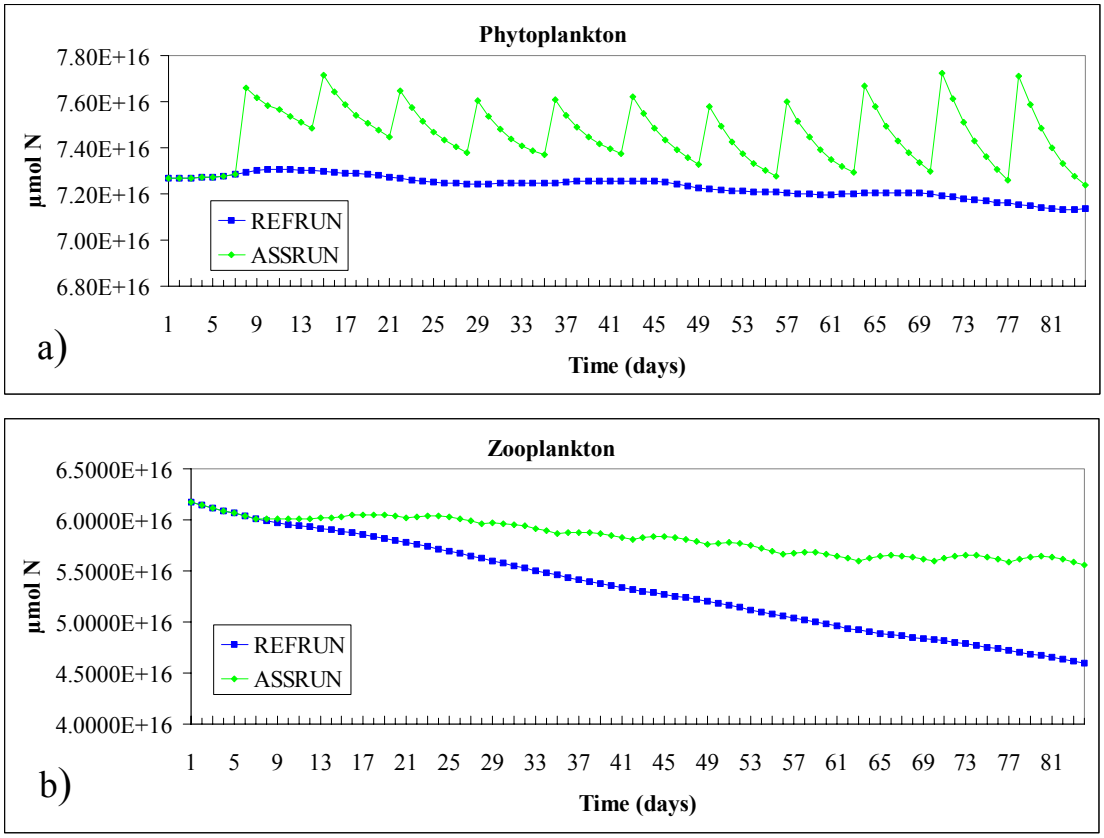

Figure 8.5. *Phytoplankton (a) and zooplankton (b) content from surface to bottom in the Mediterranean Sea, considering reference run (blu dots) and assimilated run (green dots).*

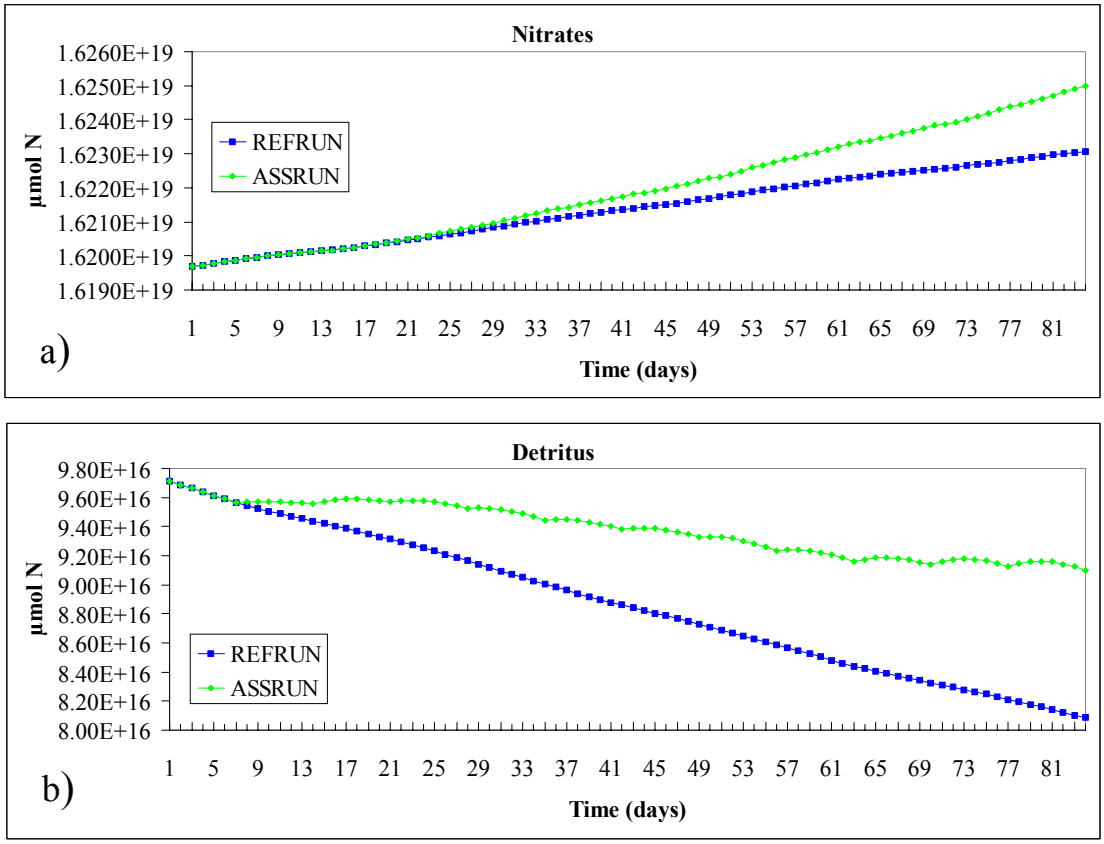

Figure 8.6. *Nitrates (a) and Detritus (b) content from surface to bottom in the Mediterranean Sea, considering reference run (blu dots) and assimilated run (green dots*

9. Conclusions and future steps

In brief, chlorophyll "sea-truth" data have been assimilated in the present 6420 FTE subtask by means of the SOFA system at 5 and 15 m, while in the first part of the Task 6400 - "Ocean Color OSSEs for the Mediterranean Sea" – surface phytoplankton has been assimilated in ITE strategy.

The aims of this task have been the use of SOFA reduced-order optimal interpolation scheme and the quantitative basis for complementing the information from the satellite ocean color. On one hand, the first of these objective can be considered reached because the surface biomass contributes significantly to improving predictability of the ecosystem description, chosen in this project as four-variables biochemical model: nutrient, primary and secondary producers, recycling compartment - detritus. On the other, a final word, for choosing the best strategy in the sense of subsurface data complementing the satellite information, requires nutrient profiles for the maintaining the total content after biological assimilation. The quantitative assessment of this influence requires consequently multivariate assimilation approaches.

Other results of this task have been an assessment of the impact of different observing data samplings. This has been obtained performing OSSEs considering different initial values of the biomass initial conditions of the winter reference run; summer biomass initial conditions for the free run; summer biomass initial conditions for the different assimilation runs.

The surface constraints induce better phytoplankton forecasts in the assimilation run with respect to the free one for FTE. Root mean square deviations are generally smaller for Z, N, D parameters after biomass assimilation. Sometimes, the evidences come from the ITE, upper layer total nitrogen shows deteriorating relative errors in eutrophic areas.

As future steps, the horizontal covariance error has to be inferred starting from the quantification of experimental chlorophyll error. The "sea-truth" satellite data

should come from fraternal models developed in MFSTEP, and the real satellite data from CZCS and SEAWIFS.

Moreover the biomass error, to be specified in the assimilation algorithm, should be represented by mapping of chlorophyll into equivalent-nutrient concentrations. The vertical covariances should be defined as EOFs from historical model run and the following two questions emerge.

Question 1: Can the chlorophyll superficial input recover the effects of high frequency specific events using the high frequency-HF transport of the hydrological model?

Question 2: How much must the chlorophyll assimilation be sustained by nutrient profiles, particularly nitrates and phosphates, to reobtain the ecosystem HF variability after few hours?

The best strategy to solve these two important questions it to concentrate upon real events as those observed in the mid April 2002 at the Cretan Sea; to set the process study with the best present ecosystem model; to assimilate recent HF satellite color data; to perform consistent numerical experiments.

Moreover the multivariate EOFs should be computed using different data sets: the temporal mean of all fields are subtracted from daily fields, and therefore EOFs represent the temporal variability of fields. In the selected biological model EOFs have to represent the error covariances between chlorophyll, nutrients, and oxygen.

In order to improve the accuracy of EOFs it could be necessary to calculate them separately in different geographical regions. For the physical parameters they should be subjectively selected using the knowledge about the properties of the water masses; for the biogeochemistry they are affairs of trial and error.

Acknowledgements

We wish to thank Fabio Raicich for his aid and encouragement in the frame of the Workpackage 6 of the European Commission Project MFS Toward Environmental Predictions, EVH3-CT-2002-00075.

References

- ADIOS, 2003. CD-ROM with 3D eco-hydrodynamical model outputs of downward fluxes and model code (MOM-based with coupled biological submodel), edited by A. Crise, G. Crispi and M. Pacciaroni. EVK3-2000-00604, D40, pp. 4 and CD-ROM.

- Allen, J. I., 2002. Simulating the Spring Phytoplankton Bloom in the Humber Plume (UK) with a variable carbon:chlorophyll-a model. In: Operational Oceanography; implementation at the European and regional scales, edited by N. Fleming. Proceedings of the II EuroGOOS Conference, Elsevier, 497-504.

- Berland, B. R., Benzhitski, A. G., Burlakova, Z. P., Georgieva, L. V., Izmestieva M. A., Kholodov, V. I. and Maestrini, S. Y., 1988. Conditions hydrologiques estivales en Méditerranée, repartition du phytoplancton et de la matière organique. Oceanol. Acta, 9(SP), 163-177.

- Bethoux, J. P., 1979. Budgets of the Mediterranean Sea. Their dependence on the local climate and on the characteristics of the Atlantic waters. Oceanol. Acta, 2(2), 157-163.

- Bryden, H. and Kinder, T. H., 1991. Steady two-layer exchange through the Strait of Gibraltar. Deep-Sea Res., 38(Suppl. 1), 445-463.

- Carrada, G., Hopkins, T., Jeftié, Lj. and Morcos, S., (editorial committee), 1983. Quantitative analysis and simulation of Mediterranean coastal ecosystems: The Gulf of Naples, a case study. UNESCO Reports in Marine Sciences, 20, pp. 158.

- *Chai F., Dugdale R. C., Peng T.-H., Wilkerson F. P. and Barber R. T., 2002. One-dimensional ecosystem model of the equatorial Pacific upwelling system. Part I: model development and silicon and nitrogen cycle. Deep-Sea Res. II, 49, 2713-2745.*

- *Civitarese, G., Crise, A., Crispi, G. and Mosetti, R., 1996. Circulation effects on nitrogen dynamics in the Ionian Sea. Oceanol. Acta, 19(6), 609-622.*

- *Cloern, J. E., Grenz, C. and Vidergar-Lucas, L., 1995. An empirical model of the phytoplankton chlorophyll:carbon ratio – the conversion factor between productivity and growth rate. Limnol. Oceanol., 40(7), 1313-1321.*

- *Coste, B., Le Corre, P. and Minas, H. J., 1988. Re-evaluation of the nutrient exchanges in the Strait of Gibraltar. Deep-Sea Res., 35, 767–775.*

- *Crispi, G., Bournaski, E. and Crise, A., 2003. Biomass assimilation in coupled ecohydrodynamical model of the Mediterranean Sea. Geoph. Res. Abstr., 15, 01215.*

- *Crispi G. and Pacciaroni, M, 2004. Reduced-order optimal interpolation for biomass data assimilation. Project MFSTEP WP6-D5. OGS Report 66/OGA-26, pp. 40.*

- *Crispi G. and Pacciaroni, M, 2005. Towards the nitrate balancing of the Mediterranean Sea: perspective through combination of loads estimate and ecosystem modeling, IMEMS 2005 Proceedings, The 8th International Marine Environmental Modeling Seminar, Helsinki Finland, 23-25 August 2005, 21.*

- *De Mey, P. and Benkiran, M., 2002. A Multivariate Reduced-order Optimal Interpolation Method and its Application to the Mediterranean Basin-scale Circulation. In: Ocean Forecasting: conceptual basis and applications, edited by N. Pinardi and J. Woods. Springer-Verlag, 281-306.*

- *Demirov, E. and Pinardi, N., 2002. Simulation of the Mediterranean Sea circulation from 1979 to 1993: Part I. The interannual variability. J. Mar. Syst., 33-34, 23-50.*

- *Doney S. C., Glover D. M. and Najjar R. G., 1996. A new coupled, one-dimensional biological-physical model for the upper ocean: Application to the JGOFS Bermuda Atlantic Time-series Study (BATS) site. Deep-Sea Res. II, 43(2-3), 591-624.*

- *Durrieu de Madron, X., Denis, L., Diaz, F., Garcia, N., Guieu, C., Grenz, C., Loÿe-Pilot, M.D., Ludwig, W., Moutin, T. and Raimbault, P., 2001. Freshwater and freshwater nutrient sources Gulf f Lions, France. Web page, http://data.ecology.su.se.*

- *Geider, R. J., MacIntyre, H. and Kana, T. M., 1996. A dynamic model of photoadaptation in phytoplankton. Limnol. Oceanol., 41, 1-15.*

- *Geider, R. J., MacIntyre, H. and Kana, T. M., 1997. Dynamic model of phytoplankton growth and acclimation: responses of the balanced growth rate and the chlorophyll a:carbon ratio to light, nutrient limitation and temperature. Mar. Ecol. Progr. Ser., 148, 187-200.*

- *Guerzoni, S., Chester, R., Dulac, F., Herut, B., Loye-Pilot, M.D., Measures, C., Migon, C., Molinaroli, E., Moulin, C., Rossini, P., Saydam, C., Soudine, A. and Ziveri, P., 1999. The role of atmospheric deposition in the biogeochemistry of the Mediterranean Sea. Progr. Oceanogr., 44(1–3), 147–190.*

- *Hamza, W., 2001. The Phenomenology of the Mediterranean Egyptian Coastal Area. MFSPP Report, Web page, www.pml.ac.uk/ecomodels/oldpages/Egypt.htm.*

- *Harzallah, A., Cadet, D. L., Crepon, M., 1993. Possible forcing effects of net evaporation, atmospheric pressure, and transients on water transports in the Mediterranean Sea. J. Geophys. Res., 98(C7), 12,341-12,350.*

- *Hood, R. R., Bates, N. R., Capone, D. G. and Olson, D. B., 2001. Modeling the effect of nitrogen fixation on carbon and nitrogen fluxes at BATS. Deep-Sea Res. II, 48, 1606-1648.*

- *Korres, G., Pinardi, N. and Laskaratos, A., 2000. The Ocean Response to Low-Frequency Interannual Variability in the Mediterranean Sea. Part I: Sensitivity Experiments and Energy Analysis. J. Clim., 13, 705-731.*

- *Lacombe, H., 1971. Le détroit de Gibraltar, océanographie physique. Notes Mém. Serv. Géol. Maroc, 222 bis, 111-146.*

- *Manca, B., Burca, M., Giorgetti, A., Coatanoan, C., Garcia, M.-J. and Iona, A., 2004. Physical and biochemical averaged vertical profiles in the Mediterranean regions: an important tool to trace the climatology of water masses and to validate incoming data from operational oceanography. J. Mar. Syst., 48(1-4), 83-116.*

- *McGill, D. A., 1970. Mediterranean Sea Atlas – distribution of nutrient chemical properties. Woods Hole Oceanographic Institution Woodshole MA.*

- *MFSTEP WP6-D5, November 2004. Reduced-order optimal interpolation for biomass data assimilation, edited by G. Crispi and M. Pacciaroni, OGS Report 66/OGA-26, pp. 40.*

- *Monaco, A. and Peruzzi, S., 2002. The Mediterranean Targeted Project MATER – a multiscale approach of the variability of a marine system – overview. J. Mar. Syst., 33-34, 3-21.*

- *Pinardi, N., Baretta, J. W., Bianchi, M., Crépon, M., Crise, A., Rassoulzadegan, F., Thingstad, F., and Zavatarelli, M., 1997. Coupled physical-biogeochemical models, in: Interdisciplinary research in the Mediterranean Sea, edited by E. Lipiatou, EUR 17787, 316-342.*

- *Osborne, J., Swift, J. and Flinchem, E. P., 1992. OceanAtlas for MacIntosh©. National Science Foundation.*

- *Pacanowski, R., Dixon, K. and Rosati, A., 1991. The G.F.D.L. Modular Ocean Model Users Guide. GFDL Ocean Group Technical Report #2. NOAA/Geophysical Fluid Dynamics Laboratory Princeton NJ.*

- *Prunet, P., Minster, J.-F., Echevin, V. and Dadou, I., 1996. Assimilation of surface data in a one-dimensional physical-biogeochemical model of the surface ocean 2. Adjusting a simple trophic model to chlorophyll, temperature, nitrate, and pCO_2 data. Global Biogeoch. Cycles, 10(1), 139-158.*

- *Raicich, F. and Rampazzo, A., 2003. Observing System Simulation Experiments for the assessment of temperature sampling strategies in the Mediterranean Sea. Ann. Geoph., 21, 151-165.*

- *Redfield, A. C., Ketchum, B. H. and Richards, F., 1963. The influence of Sea Water. In: The Sea, vol. 2, edited by M. N. Hill. Interscience, New York, pp. 26–77.*

- *Roussenov, V., Stanev, E., Artale, V. and Pinardi, N., 1995. A seasonal model of the Mediterranean Sea general circulation. J. Geoph. Res., 100(C7), 13,515-13,538.*

- *Sarmiento, J. L., Herbert, T. and Toggweiler, J. R., 1988. Mediterranean nutrient balance and episodes of anoxia. Global Biogeoch. Cycles, 2(4), 427-444.*

- *Siokou-Frangou, I., Bianchi, M., Christaki, U., Christou, E. D., Giannakourou, A., Gotsis, O., Ignatiades, L., Pagou, K., Pitta, P., Psarra, S., Souvermezoglou, E., Van Wambeke, F. and Zervakis, V., 2002. Carbon flow in the planktonic food web along a gradient of oligotrophy in the Aegean Sea (Mediterranean Sea). J. Mar. Syst., 33–34, 335–353.*

- *Slagstad D., 1982. A model of phytoplankton growth – effects of vertical mixing and adaptation to light, 3(2), 111-130.*

- *Spitz, Y. H., Moisan, J. R. and Abbott, M. R., 2001. Configuring an ecosystem model using data from the Bermuda Atlantic Time Series (BATS). Deep-Sea Res. II, 48(8-9), 1733-1768.*

- *Steele, J. H., 1962. Environmental control of photosynthesis in the sea. Limnol. Oceanogr., 7, 137-150.*

- *Sverdrup, H. U., Johnson, M. W. and Fleming, R. H., 1942. The Oceans: their Physics, Chemistry and General Biology. Prentice Hall New York, pp. 1087.*

- *Vidussi, F., Clausure, H., Manca, B. B., Luchetta, A. and Marty, J.-C., 2001. Phytoplankton pigment distribution in relation to upper thermocline circulation in the eastern Mediterranean Sea during winter. J. Geophys. Res., 106(C9), 19,939–19,956.*

- *Zavatarelli, M., Raicich, F., Bregant, D., Russo, D. and Artegiani, A., 1998. Climatological characteristics of the Adriatic Sea. J. Mar. Syst., 18(1-3), 227-263.*

Appendix 1 – Parameters of the SOFA system

OSSE Parameter	Definition	Value
ENOISE(nsets)	The normalized data error variance for each input dataset	0.07 μg Chl dm^{-3}
RCFORE	The forecast error covariance radii in the x- and y-directions	45. km
RCDATA	The data error covariance radii in the x- and the y-directions	10^{-6} km
TCFORE	The forecast error covariance e-folding time	10^{5} day
TCDATA	The data error covariance e-folding	10^{-6} day
RSDATA	The misfit selection radii in the x- and the y-directions	200. km
TSDATA	The misfit selection radius in time	7. day
NSEL	The maximum number of influential points which are to be selected for suboptimals objective analysis	20

Appendix 2 – Parameters of the biogeochemical model

Parameter	Definition	Value
η	Zooplankton efficiency	0.75
α	Degradation fraction	0.33
γ	Zooplankton growth	$1.157\ 10^{-5}\ s^{-1}$
δ	Zooplankton mortality	$1.730\ 10^{-6}\ s^{-1}$
k_P	Grazing half-saturation	1.0 μmol N dm^{-3}
r	Detritus remineralization rate	$1.18\ 10^{-6}\ s^{-1}$
k_N	Nitrate half-saturation	0.25 μmol N dm^{-3}
d	Phytoplankton mortality	$5.55\ 10^{-7}\ s^{-1}$
G	Maximum growth rate	$6.83\ 10^{-6}\ s^{-1}$
K_H	Horizontal turbulent diffusion	$1.5\ 10^{18}\ cm^4\ s^{-1}$
K_V	Vertical turbulent diffusion	$3.6\ cm^2\ s^{-1}$
w_D	Detritus sinking velocity	$5.8\ 10^{-3}$ cm s^{-1}
NCON	Cox turbulence iteration number	10
k_z	Light extinction coefficient	$3.4\ 10^{-4}\ cm^{-1}$
I_{opt}/I_0	Optimum light ratio	0.5